Journal Pre-proof

Stability in solution and chemoprotection by octadecavanadates(IV/V) in E. coli cultures

Kahoana Postal, Francielli S. Santana, David L. Hughes, André L. Rüdiger, Ronny R. Ribeiro, Eduardo L. Sá, Emanuel M. de Souza, Jaísa F. Soares, Giovana G. Nunes
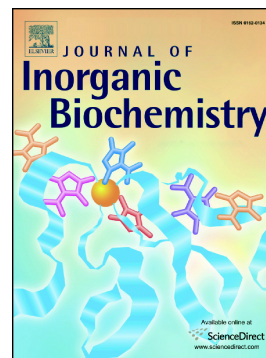
Please cite this article as: K. Postal, F.S. Santana, D.L. Hughes, et al., Stability in solution and chemoprotection by octadecavanadates(IV/V) in E. coli cultures, *Journal of Inorganic Biochemistry* (2018), https://doi.org/10.1016/j.jinorgbio.2021.111438

This is a PDF file of an article that has undergone enhancements after acceptance, such as the addition of a cover page and metadata, and formatting for readability, but it is not yet the definitive version of record. This version will undergo additional copyediting, typesetting and review before it is published in its final form, but we are providing this version to give early visibility of the article. Please note that, during the production process, errors may be discovered which could affect the content, and all legal disclaimers that apply to the journal pertain.

Stability in solution and chemoprotection by octadecavanadates(IV/V) in *E. coli* cultures

Kahoana Postal[1], Francielli S. Santana[1], David L. Hughes[3], André L. Rüdiger,[1] Ronny R. Ribeiro[1], Eduardo L. Sá[1], Emanuel M. de Souza[2], Jaísa F. Soares[1], Giovana G. Nunes[1]

[1]Departamento de Química, [2]Departamento de Bioquímica e Biologia Molecular, Universidade Federal do Paraná, Curitiba-PR, Brazil.
[3]School of Chemistry, University of East Anglia, Norwich NR4 7TJ, UK.

Corresponding Author

Giovana G. Nunes – Departamento de Química, Universidade Federal do Paraná, Centro Politécnico, Jardim das Américas, 81530-900, Curitiba-PR, Brazil. orcid.org/0000-0001-7052-2523; E-mail: nunesgg@ufpr.br

ABSTRACT

Two mixed-valence octadecavanadates, $(NH_4)_2(Me_4N)_5[V^{IV}_{12}V^{V}_6O_{42}I] \cdot Me_4NI \cdot 5H_2O$ (**V$_{18}$I**) and $[\{K_6(OH_2)_{12}V^{IV}_{11}V^{V}_7O_{41}(PO_4) \cdot 4H_2O\}_n]$ (**V$_{18}$P**), were synthesized and characterized by single-crystal X-ray diffraction analysis and FTIR, Raman, ^{51}V NMR, EPR and UV/Vis/NIR spectroscopies. The chemoprotective activity of **V$_{18}$I** and **V$_{18}$P** towards the alkylating agent diethyl sulfate was assessed in *E. coli* cultures. The complex **V$_{18}$I** was nontoxic in concentrations up to 5.0 mmol L^{-1}, while **V$_{18}$P** presented moderate toxicity in the concentration range 0.10 - 10 mmol L^{-1}. Conversely, a *ca.* 35% enhancement in culture growth as compared to cells treated only with diethyl sulfate was observed upon addition of **V$_{18}$I** (0.10 to 2.5 mmol L^{-1}), while the combination of diethyl sulfate with **V$_{18}$P** increased the cytotoxicity presented by diethyl sulfate alone. ^{51}V NMR and EPR speciation studies showed that **V$_{18}$I** is stable in solution, while **V$_{18}$P** suffers partial breakage to give low nuclearity oxidometalates of vanadium(V) and (IV). According to the results, the chemoprotective effect depends strongly on the direct reactivity of the polyoxidovanadates (POV) towards the alkylating agent. The reaction of diethyl sulfate with **V$_{18}$I** apparently produces a new, rearranged POV instead of poorly-reactive breakage products, while **V$_{18}$P** shows the formation and subsequent consumption of low-nuclearity species. The correlation of this chemistry with that of other mixed-valence polyoxidovanadates, $[H_6V^{IV}_2V^{V}_{12}O_{38}PO_4]^{5-}$ (**V$_{14}$**) and $[V^{IV}_8V^{V}_7O_{36}Cl]^{6-}$ (**V$_{15}$**), suggests a relationship between stability in solution and chemoprotective performance.

Graphical Abstract

Diethyl sulfate

$\{V_{18}O_{42}X\}^{n-}$

E. coli

$[V_{18}O_{42}I]^{7-}$

$[V_{18}O_{41}(PO_4)]^{6-}$
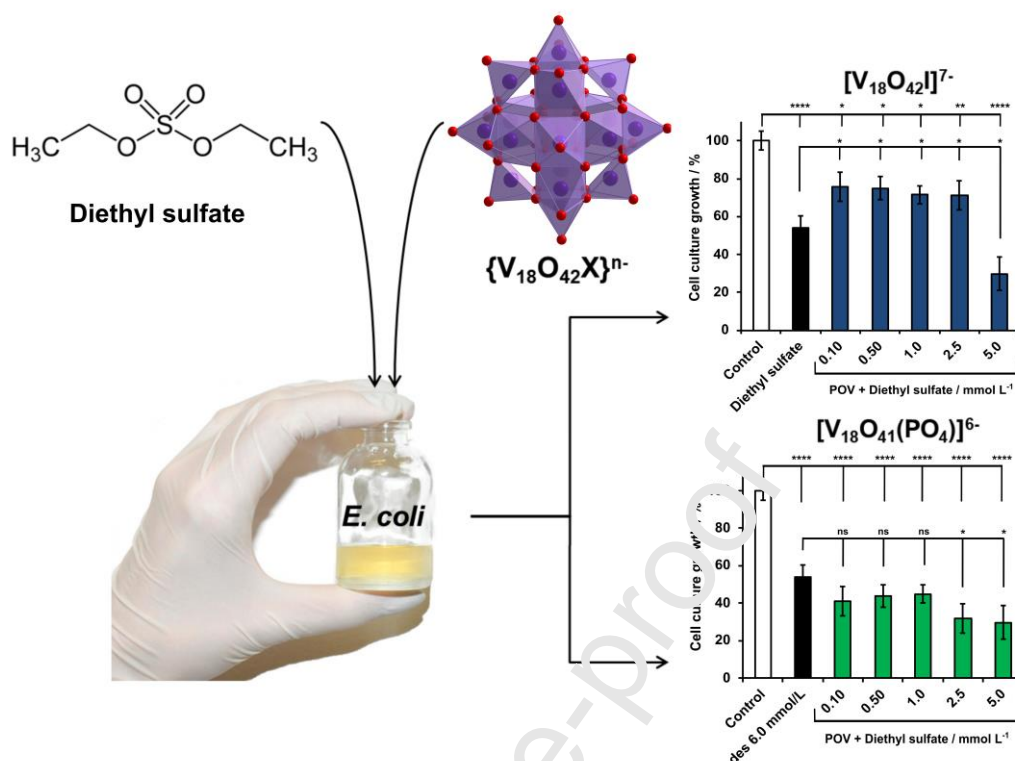
Graphical Abstract (synopsis)

The chemoprotective activity of the mixed-valence octadecavanadates $[\{K_6(OH_2)_{12}V^{IV}_{11}V^{V}_{7}O_{41}(PO_4)\cdot 4H_2O\}_n]$ (**V$_{18}$P**) and $(NH_4)_2(Me_4N)_5[V^{IV}_{12}V^{V}_{6}O_{42}I]\cdot Me_4NI\cdot 5H_2O$ (**V$_{18}$I**) against diethyl sulfate was assessed in *E. coli* cultures. **V$_{18}$I** counteracts the alkylating agent more efficiently than **V$_{18}$P**. Speciation studies suggest that chemoprotection relates to the ability of polyoxidovanadates to rearrange in solution following reaction with diethyl sulfate.

Keywords: polyoxidovanadates; alkylation; diethyl sulfate; chemoprotection; speciation

1. Introduction

Vanadium compounds have attracted attention in cardioprotection [1], as insulin-mimetics [2] and in their antihypertensive [3], antibacterial [4] [5], antiprotozoal [6, 7], antitumor [8-10] and antiviral [3, 5, 11] activities. They are also involved in DNA repair systems, acting as

antioxidant agents [12] and in the prevention of genomic instability [13, 14]. In these studies, vanadium is usually employed in the physiologically-relevant oxidation states +IV and +V.

Vanadyl sulfate ($VOSO_4$) [15] and simple vanadates, such as NH_4VO_3 and Na_3VO_4 [16-18], were effective against the deleterious effect of the DNA alkylating agents diethylnitrosamine (den) [17] and 1,2-dimethylhydrazine (1,2-dmh) [16] in mice models. A large number of vanadium compounds has been evaluated for this purpose both *in vitro* and *in vivo*, including a vanadium(III)-L-cysteine complex that exerted efficient protection against hepatotoxicity and genotoxicity induced by cyclophosphamide [19]. Another recent study on the chemoprotective activity of vanadium compounds includes the attenuation of cisplatin-induced damage in bone marrow cells of Swiss albino mice [19, 20]. In that system, the vanadium complexes increased cell proliferation; this action was attributed to the restoration of oxidized and reduced glutathione levels, decrease in free radical generation (reactive oxygen species), and enhancement of antioxidant and detoxifying enzyme levels [20].

It was additionally shown that aqueous solutions of Na_3VO_4 [21] and $[V_{15}O_{36}Cl]^{6-}$ (**V_{15}**) [22] inhibit plasmid DNA alkylation caused by diethyl sulfate, $(C_2H_5O)_2SO_2$, by up to 40% and 70%, respectively. **V_{15}** was also effective against dimethyl sulfate, a more potent alkylating agent, showing a 48% protective effect on pUC19 DNA. The mechanism of chemoprotection remains elusive, but the most accepted proposal suggests that the oxidometalates act as nucleophiles and compete with the DNA for the alkylation agent [21-24]. Recently, *E. coli* cultures exposed to diethyl sulfate were applied as whole-cell models to evaluate the chemoprotective ability of oxidovanadium compounds. The activities of $[H_6V_{14}O_{38}PO_4]^{5-}$ (**V_{14}**) and **V_{15}** were antagonistic [25], and seem to depend on both the stability of the polyoxidovanadate in solution and its capability to rearrange or form new aggregates after reaction with the alkylating agent [22, 23, 25]. These systems exemplify the remarkable

complexity of the chemoprotective effect exerted by the polyoxidovanadates, and further investigation of the relationship between stability in solution and activity in *E. coli* cells, as a pre-established biological model to allow comparison, appeared essential.

Compounds with structurally equivalent $V_{18}O_nX$ shells (n = 36-44; X = encapsulated species such as Cl^-, Br^-, I^-, PO_4^{3-}, SO_4^{2-}, SO_3^{2-}, VO_4^{3-}, NO^{2-}, NO_3^-, SH^-, $HCOO^-$, CO_3^{2-} and H_2O) show a more variable host-guest chemistry as compared to other polyoxidovanadates [26-30]. Additionally, a study reported by Müller and co-authors [26] revealed that high-nuclearity aggregates such as $V_{18}O_{42}X$ present different $V^{IV}:V^V$ ratios, this variability led to interesting structural, spectroscopic, magnetic [26], electronic [27, 31] and catalytic properties [32, 33]. Recently, the compounds $[V_{18}O_{42}(H_2O)]^{12-}$ [34] and $[V_{18}O_{44}(N_3)]^{10-}$ [35] demonstrated good antitumoral and anti-proliferative efficacy against human melanoma and breast, cervical and lung cancer [36]; however, the two mixed-valence polyoxidovanadates encapsulating phosphate and azide were less explored. Because of their high compositional and structural variability, octadecavanadates constitute an interesting platform to study the effect of anion encapsulation and metal oxidation states (+IV and +V) on the chemoprotection effect.

Herein, a methodology to synthesize two mixed-valence polyoxidovanadates (MV-POV), $(NH_4)_2(Me_4N)_5[V^{IV}_{12}V^V_6O_{42}I]\cdot Me_4NI\cdot 5H_2O$ (**V$_{18}$I**) and $[\{K_6(OH_2)_{12}V^{IV}_{11}V^V_7O_{41}(PO_4)\cdot 4H_2O\}_n]$ (**V$_{18}$P**), is presented; the complexes are variations of the classical core-shell octadecavanadates described by Müller [26]. Both products were characterized in the solid-state and aqueous solutions. **V$_{18}$P** crystallizes as a one-dimensional chain of oxido-bridged $PO_4@V_{18}O_{42}$ units; to the best of our knowledge, such a polymeric framework for octadecavanadates is unprecedented in the literature. As far as V_{18} units are concerned, although $\{V^{IV}_{12}V^V_6O_{42}I\}^{7-}$ and $\{V^{IV}_{11}V^V_7O_{42}(PO_4)\}^{6-}$ have already been reported, the products here described differ from them in the proportion of V^{IV} to V^V, combination with the counterions and number of water molecules

in the unit cell. The present work aimed to contribute both to the establishment of structural and reactivity patterns for polyoxidovanadates, and to the prevention of the damage caused by alkylating agents to living organisms. In this context, the chemoprotective capability of $\mathbf{V_{18}I}$, $\mathbf{V_{18}P}$, and $[V_{10}O_{28}]^{6-n}$ ($\mathbf{V_{10}}$) towards whole cells was evaluated in *E. coli* cultures. The results were correlated with those given by the direct reaction of the polynuclear complexes with diethyl sulfate, monitored by ^{51}V NMR and EPR spectroscopies, and with our previous findings with $\mathbf{V_{14}}$ and $\mathbf{V_{15}}$ in similar experimental and biological conditions.

2. Experimental

2.1. Chemicals and solutions

Ultrapure water (MilliQ, Millipore type , 18.2 MΩ·cm resistivity at 25 °C) was used in the syntheses. Me$_4$NI (99.0%), diethyl sulfate (98.0%) and deuterium oxide (99.9%) were purchased from Aldrich; NH$_4$VO$_3$ (99.0%) from Vetec; mannitol (99.2%) from USB. Sodium decavanadate [{Na$_6$(OH$_2$)$_{20}$V$_{10}$O$_{28}$·4H$_2$O}$_n$] was synthesized as described elsewhere [37] and its aqueous solution (14.3 mmol L^{-1}, pH = 4) was prepared immediately before use.

2.2. Analytical methods

Elemental analyzes were run by MEDAC Laboratories Ltd. (Chobham, Surrey, UK). Carbon, hydrogen, and nitrogen contents were determined by combustion on a Perkin Elmer CHN 2400 Elemental Analyzer; V and K contents were obtained by Inductively Coupled Plasma-Atomic Emission Spectroscopy (ICP-OES) with a Varian Vista MPX ICP-OES system. Infrared spectra (4000 – 400 cm^{-1}) were measured from KBr pellets on an FTIR MB-BOMEN spectrophotometer. Raman spectra were obtained using Ar$^+$ (514 nm) and He-Ne (632.8 nm)

laser excitation in the range of 200 to 4000 cm^{-1}, with incident power of 0.20 mW; the equipment was a Renishaw Image spectrophotometer with an optical microscope that focuses the incident radiation on a 1 mm^2 area. Magnetic susceptibilities were measured in the solid-state at 296 K with a modified Gouy method [38, 39] using a Johnson-Matthey MKII magnetic susceptibility balance. Ultra-pure water and $(NH_4)_2Fe(SO_4)_2·12H_2O$ were used as calibration standards, and corrections for the diamagnetism of the ligands employed Pascal constants [40] (χ_{DIA} for $C_{24}H_{90}I_2N_8O_{47}V_{18} = -1020.2×10^{-6}$ cm^3 mol^{-1}, and for $H_{32}K_6O_{61}PV_{18} = -925.6×10^{-6}$ cm^3 mol^{-1}). UV/Vis/NIR spectra (250 – 2500 nm) were acquired on a PerkinElmer LAMBDA 1050 UV/Vis/NIR spectrophotometer equipped with a PMT/InGaAs/PbS three-detector setup. The aqueous samples were prepared at room temperature with concentrations from 0.01 to 2.0 mmol L^{-1}. X-band EPR spectra (9.5 GHz) were recorded at room temperature and 77 K from pulverized solid and solutions in water and Luria-Bertani medium using a Bruker EMX-Micro spectrometer. Spectral simulations were run with the EasySpin software [41] and intensities of signals were normalized with a chromium(III) (Cr^{3+}@MgO) standard. Thermogravimetric (TGA) data were collected on a Netzsch STA449 F3 Jupiter analyzer equipped with a silicon carbide furnace and dinitrogen as the carrier gas. Samples (*ca.* 4 mg) were heated in aluminum pans from 25 – 800 °C at 10 °C min^{-1}. ^{51}V NMR spectra were acquired at 295 K in aqueous solutions containing 10% D_2O, prepared approximately 10 to 30 min before analysis. Spectra were recorded on a Bruker 400 MHz Avance III spectrometer (9.4 T) equipped with a multinuclear direct detection probe (5 mm), using calibrated 90° pulses, 2048 scans, a recycling delay of 0.100 s, acquisition times of 0.16 s and a spectral width of 990 ppm (+44 to –946 ppm). ^{51}V was detected at 105.2 MHz using VOCl$_3$ (neat, capillary, 0.00 ppm) as a reference. Spectral intensities were normalized on each experiment by comparison with the reference signal.

2.3. Preparation of $[\{K_6(OH_2)_{12}V^{IV}_{11}V^V_7O_{41}(PO_4)·4H_2O\}_n]$ (*phosphate@octadecavanadate,* **V$_{18}$P**)

The reaction was carried out with 0.836 g of NH_4VO_3 (7.20 mmol), 0.660 g of mannitol (3.60 mmol), and 0.490 g of KH_2PO_4 (3.60 mmol) dissolved with heating in 50 mL of water. The dark green resulting solution was left to cool down to the room temperature, and the pH was adjusted to 9.40 with KOH. The mixture was then stirred under reflux for 48 hours, resulting in a bluish-green solution. After two days at 4 °C, 0.277 g of deep green crystals ($V_{18}P$) were isolated and washed with cold water and ethanol, giving a 30% yield based on NH_4VO_3. Alternatively, mannitol was replaced by DL-malic acid (0.482 g, 3.60 mmol) in the same route, producing 0.546 g of the deep green crystals of $V_{18}P$ (62% yield based on NH_4VO_3). Product $V_{18}P$ was soluble in water and insoluble in polar and nonpolar organic solvents. Elemental analysis contents calculated for $H_{32}K_6O_{61}PV_{18}$ were H 1.47; K 10.71; P: 1.41; V 41.89%. Found: H 1.21; K 10.48; P 1.17; V 41.78. Taken together and within experimental error, all characterization results presented in this and the following sections indicate $[\{K_6(OH_2)_{12}V^{IV}_{11}V^{V}_{7}O_{41}(PO_4)\cdot4H_2O\}]$ as the best total formulation for the product. FTIR (cm^{-1}, s = strong, m = medium, and w = weak): 3390(s), 1618(m), 1054(w), 980(s), 932(s), 797(w), 673(w), 582(w).

2.3.1. *Single-crystal X-ray diffraction analysis of* $V_{18}P$

A suitable dark green crystal of $V_{18}P$ (*ca* 0.352 x 0.085 x 0.046 mm) was mounted on a Bruker D8 Venture diffractometer equipped with a Photon 100 CMOS detector, Mo–Kα radiation and graphite monochromator. From a sample under oil, one crystal was taken, mounted on a MicroMount/micromesh assembly™ (MiTeGen), and fixed on the goniometer head. Data were processed using the APEX3 program [42]. The structure was determined by the intrinsic phasing routines in SHELXT [43] and refined by full-matrix least-squares methods, on F^2's, in SHELXL. Computer programs were run through WinGX [44]. The non-hydrogen atoms were

refined with anisotropic thermal parameters. The structure diagrams were drawn with ORTEP3 and Diamond 4 software [45]. After convergence of the refinement of the V_{18} aggregate including the potassium counterions, the main residual electron density peaks were assigned to isolated oxygen atoms from the extensively disordered water molecules. Hydrogen atoms were not located in the Fourier difference map due to this high degree of crystallographic disorder, which can also explain the holes of electron density.

Crystal data and crystallographic details for **$V_{18}P$** are collated in Table S1.

2.4. Preparation of $(NH_4)_2(Me_4N)_5[V^{IV}_{12}V^V_6O_{42}I] \cdot Me_4NI \cdot 5H_2O$

(*iodide@octadecavanadate*, **$V_{18}I$**)

The reaction was carried out with 0.836 g of NH_4VO_3 (7.20 mmol), 0.656 g of mannitol (3.60 mmol), and 0.668 g of Me_4NI (4.80 mmol) dissolved in 50 mL of water. The mixture was boiled under reflux for 24 hours, resulting in a deep green solution that was cooled down and kept at 4 °C. After three weeks, deep green crystals of **$V_{18}I$** were filtered off, exhaustively washed with cold water and ethanol, and dried under vacuum to give 0.611 g of product (69% yield based on NH_4VO_3). **$V_{18}I$** is soluble in water and insoluble in polar and nonpolar organic solvents. Elemental analysis contents calculated for $C_{24}H_{90}I_2N_8O_{47}V_{18}$: C 11.94; H 3.76; N 4.64; V 37.99%; I 10.52%. Found: C 11.85; H 3.47; N 4.27; V 37.73%: I 10.24%. This elemental composition was reproducibly obtained for distinct batches of the product isolated from independent preparations. It differs from the results of single crystal X-ray diffraction analysis by the presence of additional $(Me)_4NI$, and is also supported by thermogravimetric analysis, as discussed below. FTIR (KBr, cm^{-1}): 3461(s), 1635(w), 1483(s), 1398(w), 986(s), 738(w), 627(w). Raman (cm^{-1}): 155(s), 267(w), 415(w), 516(w), 669(w), 1021(w).

Crystal data for $V_{18}I$. A dark green crystal of $\mathbf{V_{18}I}$ (*ca* 0.207 x 0.198 x 0.152 mm) was selected and mounted on a Bruker D8 Venture diffractometer equipped with a Photon 100 CMOS detector, Mo–Kα radiation and graphite monochromator. Data collection was carried out at 100(2) K, and data processing, structure resolution, and refinement were performed as described for $\mathbf{V_{18}P}$. In the case of $\mathbf{V_{18}I}$, the refinement of the counterions was not possible due to the poor quality of the crystals, leading, in consequence, to high residual electron density and high values of the statistical parameters R_1, wR_2, and goodness-of-fit (R_1(all data) = 0.2091; wR_2(all data) = 0.6213; goodness-of-fit = 3.614). Atoms O1w and O2w were assigned to water molecules that crystallized together with the polynuclear aggregate; their hydrogen atoms were not located in the Fourier difference map due to the high degree of disorder in the system. The $\mathbf{V_{18}I}$ product crystallized in the cubic space group Fm-3m, with unit cell parameters $a = b = c = 19.4906(8)$ Å, $α = β = γ = 90°$, $V = 7404.2(9)$ Å^3; $Z = 4$, $d = 1.068$ mg m^{-3}, F(000) = 3500, T = 100(2) K, μ(Mo-Kα) = 2.646 mm^{-1}, λ(Mo-Kα) = 0.7103 Å.

2.5. Biological assays

The effect of the V_{18} polyoxidovanadates on the alkylation caused by diethyl sulfate was evaluated in *E. coli* (strain DH5α) using a protocol described in our previous work [25]. The optical densities of all cultures were read at 595 nm (OD$_{595}$) to avoid the absorption bands typical of the culture media and those observed in the electronic spectra of the POV. The solutions of the $\mathbf{V_{18}I}$ and $\mathbf{V_{18}P}$, in the same concentrations applied in the assays, were used as blanks. Cells were kept in glycerol 50% at –20 °C before seeding in Luria agar plates containing 10 μg mL^{-1} of nalidixic acid at 37 °C. The freshly-grown colonies were subsequently inoculated in liquid Luria-Bertani (LB) broth for the experiments that are described as follows.

Firstly, bacteria were grown at 37 °C and 120 rpm in 10 mL of LB medium containing 10 μg mL^{-1} of nalidixic acid until the OD$_{595}$ of the cultures reached 1.0. Cells were then

collected by centrifugation (4900×g, 10 min), resuspended, and incubated for 15 min at 37 °C in 1.0 mL of saline solution (0.90% NaCl), diethyl sulfate or POV solution depending on the specific experiment. These samples were then transferred to 5 mL of LB and incubated at 37 °C and 120 rpm for 3 h. OD_{595} measurements assessed growth.

In the case of the chemoprotection assays, the bacterial pellets were resuspended in saline solution immediately after centrifugation, and different amounts of POV (0.10, 0.50, 1.0, 2.5, 5.0 10 mmol L^{-1}) were added. Approximately one minute later, the cell suspensions received the addition of a fixed amount of diethyl sulfate (6.0 mmol L^{-1}). This concentration of the alkylating agent corresponds to GI_{50} (concentration that inhibits the growth of bacteria by 50%) as determined in our previous work [25]. All samples were then incubated for 15 min at 37 °C, transferred to 5 mL of LB, and then incubated again at 37 °C and 120 rpm. Growth was assessed after 3 h by OD_{595} measurements. The results were expressed as arithmetic averages with standard deviation of three independent experiments. Differences between multiple groups and the controls, with and without diethyl sulfate, were assessed by one-way ANOVA followed by the Tukey's multiple comparisons test [46]. A value of $P < 0.05$ was considered statistically significant.

3. Results and discussion

3.1. Syntheses

As described in our previous work, the partial reduction of metavanadate (VO_3^-) by mannitol in aqueous medium under reflux proved to be an efficient methodology for the preparation of $(Me_4N)_6[V^{IV}_8V^V_7O_{36}Cl]$ (V_{15}) in good yield [22]. We describe here the synthesis of $(NH_4)_2(Me_4N)_5[V^{IV}_{12}V^V_6O_{42}I]·Me_4NI·5H_2O$ ($V_{18}I$) by the same route, replacing the source of

the guest anion, Me$_4$NCl, by the analogous Me$_4$NI. As expected, in this case the nuclearity of the resulting mixed-valence polyoxidovanadate was determined by the size of the guest halide.

The structural framework obtained with phosphate, in turn, proved to be more susceptible to the reaction conditions. The use of KH$_2$PO$_4$ in slightly acidic medium (pH $\cong$ 6) produced K(NH$_4$)$_5$[H$_6$V$^{IV}_2$V$^V_{12}$O$_{38}$(PO$_4$)]·11H$_2$O **(V$_{14}$)** [25], while in this work [{K$_6$(OH$_2$)$_{12}$V$^{IV}_{11}$V$^V_7$O$_{41}$(PO$_4$)·4H$_2$O}$_n$] **(V$_{18}$P)** was obtained by adjusting the initial pH of the reaction mixture to 9. The influence of the reducing agent became evident by the nearly two-fold increase in **V$_{18}$P** yield when mannitol was replaced by malic acid. Indeed, the oxidation of organic molecules by vanadium(V) compounds is well known, with the kinetic rate and reduction degree depending on the acidity of the medium and nature of the organic molecules [47].

3.2. Solid-state characterization of **V$_{18}$P**

The 3D polymeric structure of **V$_{18}$P** is composed of interconnected MV-POV aggregates, each decorated with six potassium aqua complexes (Fig. 1b and Fig. S2). Lattice water molecules are also present in the repeating unit. The polyoxidoanion structure shows three structural types of vanadium, two apical, eight outer ring, and eight inner ring atoms arranged as (1×V):(4×V):(8×V):(4×V):(1×V) (Fig. S1). Details on data collection, structure refinement, and selected bonds and angles are presented in Tables 1 and S1. The bond lengths in the **V$_{18}$P** polyoxidoanion are in the same ranges described for other octadecavanadate(IV/V) aggregates [27, 33].

The phosphorus atom at the center of each POV is found in a fourfold, tetragonal site. Consequently, the two crystallographically independent oxygen atoms of the phosphate anion, O(1p) and O(2p), generate, by symmetry, a total of eight oxygen atoms in a cube; these comprise

two overlapping tetrahedral PO_4 units related by a center of symmetry at the phosphorus atom. The bond lengths of P–O(1P) and P–O(2P) are 1.553(11) and 1.530(12) Å, respectively. Each oxygen of the phosphate anion also contacts three vanadium atoms with $O_{phosphate}\cdots V$ distances in the range of 2.370 – 2.489 Å.

The structure of **V₁₈P** also includes three crystallographically independent potassium cations; they coordinate the oxygen atoms of the polyoxidoanions (Table S2) with bond lengths ranging from 2.624 to 3.062 Å. These values are similar to those reported in the literature [48]. Their coordination sphere is completed by water molecules which are assumed to be involved in an extensive hydrogen bonding network with the oxido groups of the MV-POV and other water molecules in the lattice (Fig. S2); the hydrogen atoms were not located due to crystallographic disorder.

Table 1 Selected bond lengths (Å) and angles (°) for $[\{K_6(OH_2)_{12}V^{IV}_{11}V^{V}_7O_{41}(PO_4)\cdot 2.6H_2O\}_n]$ (**V₁₈P**) with estimated standard deviations in parentheses

Bond lengths / Å					
V(1)–O(1)	1.597(6)	V(6)–O(10)	1.948(9)	O(5)-K(1)	2.736(11)
V(1)–O(11)	1.877(7)	V(6)–O(10)#3	1.948(9)	O(6)-K(1)#2	3.027(9)
V(1)–O(10)	1.896(7)	V(7)–O(5)	1.616(9)	O(7)-K(1)#2	3.399(4)
V(1)–O(12)	1.934(7)	V(7)–O(8)	1.916(7)	O(7)-K(1)#6	3.399(4)
V(1)–O(8)	1.952(7)	V(7)–O(8)#1	1.916(7)	O(10)-K(1)#2	2.771(11)
V(1)-O(1P)#1	2.453(11)	V(7)–O(9)	1.965(7)	K(1)–O(2W)#10	2.866(15)
V(2)–O(6)	1.596(6)	V(7)–O(9)#1	1.965(7)	K(2)–O(3W)	2.831(14)
V(2)–O(10)	1.875(7)	P(1)–O(2P)	1.531(10)	K(3)–O(5W)#12	2.74(4)
V(2)–O(11)#3	1.918(7)	P(1)–O(1P)	1.549(10)	K(3)–O(2W)#10	3.201(17)
V(2)–O(9)	1.941(7)	O(1P)–O(2P)#5	1.775(14)	V(1)-V(6)	2.828(2)
V(2)–O(13)	1.949(7)	O(1P)–O(1P)#1	1.78(2)	V(1)-V(3)	2.8951(19)
V(2)–O(1P)	2.441(12)	O(2P)–O(2P)#1	1.74(2)	V(1)-K(2)	3.735(4)
V(6)–O(7)	1.624(4)	O(1)–K(3)#2	2.840(8)	V(1)-K(1)#2	3.916(3)
V(6)–O(11)#3	1.919(9)	O(1)–K(2)	3.059(9)		
V(6)–O(11)	1.919(9)	O(1)–K(1)#2	3.408(9)		

Angles / °					
O(1)–V(1)–O(11)	100.4(4)	O(7)-V(6)-O(11)	110.3(3)	O(2P)-P(1)-O(2P)#1	69.4(8)
O(11)–V(1)–O(10)	85.8(4)	O(11)#3-V(6)-O(11)	139.4(7)	O(2P)-P(1)-O(2P)#3	110.6(8)
O(1)–V(1)–O(12)	101.8(4)	O(7)-V(6)-O(10)	109.7(3)	O(2P)#1-P(1)-O(2P)#3	180.0(6)
O(11)–V(1)–O(12)	93.7(4)	O(11)-V(6)-O(10)	83.2(3)	O(2P)#5-O(1P)-V(1)#1	69.4(5)
O(10)–V(1)–	157.6(4)	O(10)-V(6)-	140.6(6)	O(1P)#1-O(1P)-	131.9(2)

O(12)		O(10)#3		V(1)#1	
O(1)–V(1)–O(8)	102.1(4)	O(7)-V(6)-V(1)	118.06(8)	V(1)-O(1)-K(3)#2	161.8(4)
O(11)–V(1)–O(8)	157.5(4)	O(11)-V(6)-V(1)	41.3(2)	V(1)-O(1)-K(2)	102.1(3)
O(10)–V(1)–O(8)	90.2(3)	V(1)-V(6)-V(1)#3	123.88(16)	K(3)#2-O(1)-K(2)	94.7(2)
O(12)–V(1)–O(8)	81.8(3)	O(7)-V(6)-V(2)	117.85(8)	V(1)-O(1)-K(1)#2	96.2(3)
O(1)-V(1)-O(1P)#1	158.4(4)	O(7)-V(6)-K(1)#2	64.46(6)	K(3)#2-O(1)-K(1)#2	74.6(2)
O(11)-V(1)-O(1P)#1	64.7(4)	O(11)#3-V(6)-K(1)#2	95.6(2)	K(2)-O(1)-K(1)#2	97.1(2)
O(10)-V(1)-O(1P)#1	94.2(4)	O(11)-V(6)-K(1)#2	101.6(2)	V(6)#4-O(7)-V(6)	180.0
O(1)-V(1)-V(6)	105.2(3)	O(10)-V(6)-K(1)#2	45.4(3)	V(6)#4-O(7)-K(1)#2	90.0
O(11)-V(1)-V(6)	42.4(3)	O(10)#3-V(6)-K(1)#2	173.3(3)	V(2)-O(10)-V(6)	95.8(4)
O(12)-V(1)-V(6)	131.5(2)	K(1)#2-V(6)-K(2)	79.52(12)	V(1)-O(10)-V(6)	94.7(4)

Symmetry transformations used to generate equivalent atoms: #1 –x–1,y,–z+1; #2 –x+3/2,–y+1/2,–z+2; #3 –x+1,–y,–z+1; #4 x,–y+1,z; #5 –x+1,–y+1,–z+1; #6 x–1/2,y–1/2,z–1; #7 –x+3/2,–y+1/2,–z+1; #8 –x+3/2,y–1/2,–z+2; #9 –x+3/2,–y+3/2,–z+2; #10 x,–y,z; #11 –x+3/2,y+1/2,–z+1; #12 –x+3/2,–y–1/2,–z+1 #13 x,y–1,z; #14 x,y+1,z; #15 –x+3/2,y+1/2,–z+2; #16 x+1/2,y+1/2,z+1.
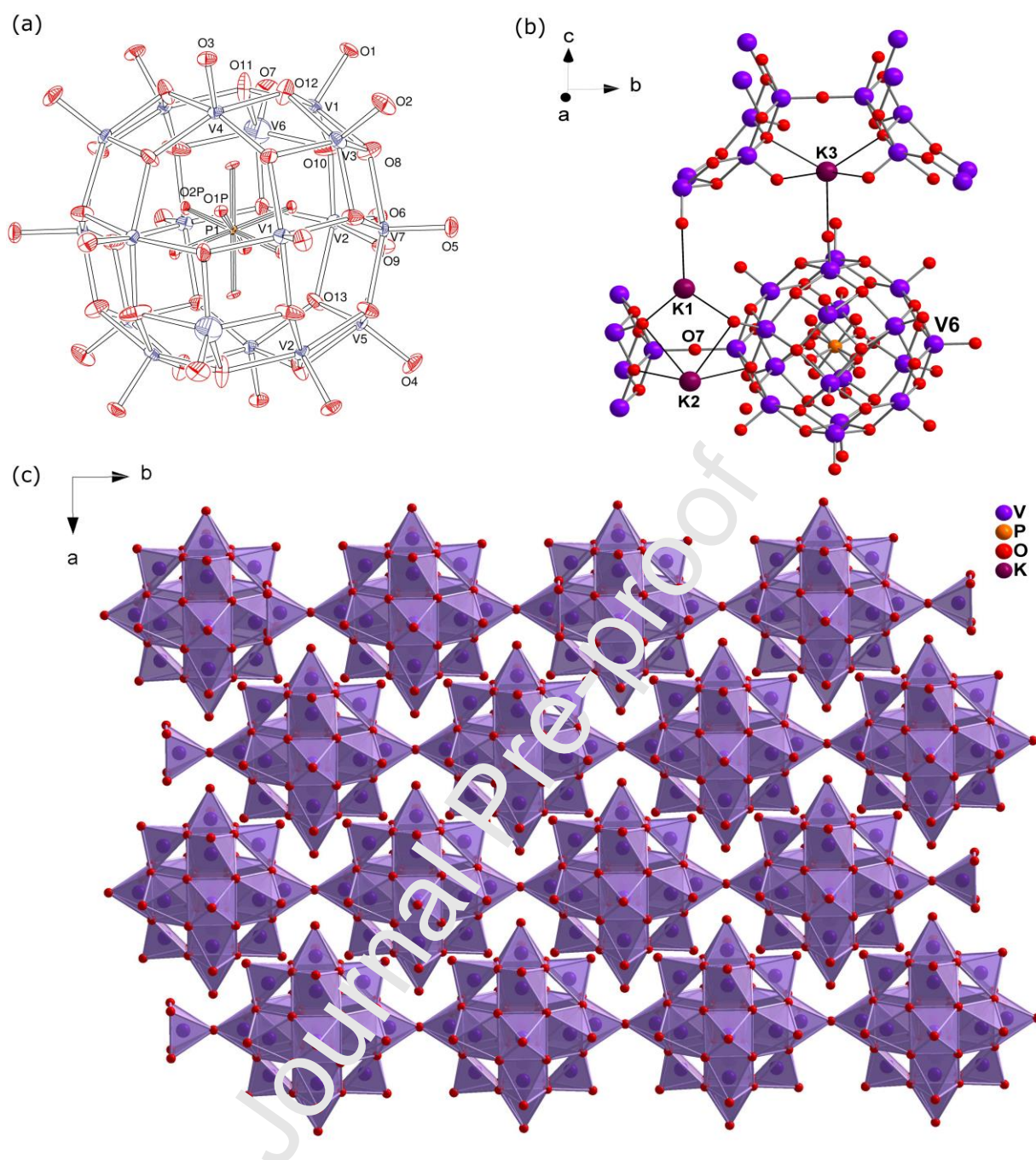
Fig. 1. *(a)* ORTEP representation of the octadecavanadate (**V$_{18}$P**) anion encapsulating a disordered phosphate. The potassium cations and the oxygen atoms from the water molecules were omitted for clarity. Thermal ellipsoids are drawn at the 30% probability level; *(b)* Coordination of potassium cations by the **V$_{18}$P** clusters; *(c)* Packing of the polyoxidoanion chains in $[\{K_6(OH_2)_{12}V^{IV}_{11}V^{V}_7O_{41}(PO_4)\cdot2.6H_2O\}_n]$ (**V$_{18}$P**), viewed in the *ab* plane. Each five-coordinate vanadium ion is represented by a purple polyhedron; one apical and four inner ring polyhedra are partially or totally hidden in this perspective view but can be implied by symmetry. The lattice counterions and water molecules were omitted for clarity.

All the vanadium centers of **V$_{18}$P** have approximately square pyramidal coordination, with the structural parameter (τ) [49] close to zero. The metal ions in the cage are bridged by μ_3-O atoms with an average bond length of 1.922(8) Å (Fig. 1a); the vanadyl bond lengths (average

value of 1.611(9) Å) fall in the same range reported for other $\{V_{18}O_{42}X\}$ aggregates [50]. A particular feature of the **$V_{18}P$** structure is the presence of oxido bridges (μ_2-O) connecting the polynuclear aggregates through linear V(6)–O(7)–V(6)^i bonds; this produces one-dimensional chains of $\{V_{18}O_{42}(PO_4)\}$ units that run parallel to the *b* direction (Fig. 1c). The V(6)–O(7) bond (1.624(4) Å, Fig. 1b) is shorter than the 1.714(6) Å value described for a similar bond in the 3-D network of $Na_6[V_{18}O_{39}(PO_4)]_2 \cdot H_3PO_4 \cdot 31H_2O$ [50]. Discrete $\{V_{18}O_{42}(PO_4)\}^{x-}$ anions reported in the literature [30, 51] present more distorted geometries for the vanadium centers, with τ values varying from 0.0 to 0.5 in the same anion. As a consequence, the **$V_{18}P$** shell described in the present work is closer to the spherical shape; accordingly, the distances between opposite vanadium centers in the cage are more similar to one another than those observed in the discrete analogs.

The solid-state EPR spectrum of **$V_{18}P$** at 77 K (Fig. S3) presents a broad line with Δ_{pp} = 36.7 mT and g = 1.974, typical of polynuclear species containing vanadium(IV) centers. The titrimetric analysis [52] of **$V_{18}P$** showed a mean metal valence of 4.44, close to the average value (4.39) for 11 vanadium(IV):7 vanadium(V) centers. This proportion is compatible with the charge balance indicated by single-crystal X-ray diffraction analysis (XRD). A similar result was given by the bond valence sum calculations [53] based on the XRD data and V–O bond lengths (Table S3), allowing for a degree of valence delocalization involving the metal sites (see infra). Magnetic susceptibility measurements carried out in the solid-state at 300 K ($\chi_M T = 1.53$ cm^3 K mol^{-1}) are compatible with the presence of antiferromagnetic exchange among the unpaired spins in the polyoxidoanion, concurring with the described for similar V_{18} aggregates [26].

3.3. Solid-state characterization of **$V_{18}I$**

Dark green crystals of **V$_{18}$I** were suitable for single-crystal XRD; however, the high level of disorder involving the water molecules and the ammonium cations in the lattice made the localization of hydrogen atoms in the Fourier map difficult. The structure of the polyoxidoanion is well defined and composed of 18 vanadyl groups, with 42 oxido groups bridging the vanadium centers (Fig. S4). This framework encapsulates one iodide ion, which lies on a center of symmetry. This topology is analogous to the superKeggin-type $\{V_{18}O_{42}I\}^{n-}$ clusters (n = 5, 11, 13) described with a D_{4d} arrangement by Müller and co-authors [26]. Titrimetric determination of vanadium(IV and V) in **V$_{18}$I** crystals gave a mean valence value of 4.28, which corroborates our proposed $(NH_4)_2(Me_4N)_5[V^{IV}{}_{12}V^{V}{}_6O_{42}I]\cdot Me_4NI\cdot 5H_2O$ formulation (calculated average 4.33). The mixed-valence nature of the polymetallic aggregate is also supported by the broad line of the **V$_{18}$I** solid state EPR spectrum at 77 K (g = 1.963 and Δ_{pp} = 24.7 mT, Fig. S5). Magnetic susceptibility measurements carried out for **V$_{18}$I** in the solid state at 292.5 K ($\chi_M T$ = 1.87 cm^3 K mol^{-1}) again suggest antiferromagnetic coupling of the unpaired electrons in the polynuclear cage, as in the case of **V$_{18}$P**. This result is intermediate between the $\chi_M T$ values reported for $(Et_4N)_5[V^{IV}{}_{10}V^{V}{}_8O_{42}I]$ ($\chi_M T$ = 0.9 cm^3 K mol^{-1}) and $K_{10}[HV^{IV}{}_{16}V^{V}{}_2O_{42}I]\cdot 16H_2O$ (2.2 cm^3 K mol^{-1}) [26].

3.4. Vibrational spectroscopies

The infrared spectra of **V$_{18}$I** and **V$_{18}$P** (Fig. S6 and Table S4) showed bands in the range of 580 to 985 cm^{-1}, characteristic of polyoxidovanadates, attributed to ν(V–O), ν(V–O–V), δ(V–O–V) and ν(V=O), and also at *ca.* 3400 and 1600 cm^{-1} for ν(O–H) of water molecules. The spectrum of **V$_{18}$I** also presented the tetramethylammonium cation bands at 1486 and 1407 cm^{-1}, assigned to δ_{as} and δ_s(CH$_3$) vibrations. **V$_{18}$P**, in turn, showed a band at 980 cm^{-1} attributed to ν(P=O), confirming the presence of the phosphate anion in the structure. The Raman spectra of both compounds present bands from 400 to 550 cm^{-1} referred to δ(V–O–V) vibration modes

(Fig. S7), while the bands in the range of 660 to 1020 cm^{-1} were assigned to ν(V–O–V) and ν(V=O) [54].

3.5. Thermogravimetric analyses (TGA)

The thermogram and derivative thermogram of **V$_{18}$P** show one step up to 200 °C that corresponds to the loss of 11 water molecules (Fig. S8a). This assignment is supported by the good agreement between the experimental and calculated mass values (8.9% and 9.0%, respectively). The loss of the five remaining water molecules can be observed up to 600°C corresponding to 4.1% of the total mass (experimental value of 4.4%). The thermal decomposition of the polyoxidovanadate framework occurs above this temperature. For **V$_{18}$I**, in turn, the thermogram shows three decomposition steps (Fig. S8b), the first from 20 to 200 °C corresponding to the loss of the five water molecules of crystallization and two ammonium cations (determined value = 5.4%; calculated value = 5.2%). The second step, up to 400 °C, refers to the loss of five tetramethylammonium cations and the additional tetramethylammonium iodide (calculated value of 23.0%, determined value = 24.0%). Such assignment agrees with the elemental analysis results and is supported by literature on the thermal decomposition of tertiary ammonium halides, which occurs in the same temperature range [55]. In the present case, the thermal decomposition of the polyoxidoanion is more complicated to rationalize than those of simple ammonium salts, and continues up to 610 °C. In summary, the TGA data, added to the results of X-ray diffraction and elemental analyses, support the formulations (NH$_4$)$_2$(Me$_4$N)$_5$[V$^{IV}_{12}$V$^V_6$O$_{42}$I]·Me$_4$NI·5H$_2$O (**V$_{18}$I**) and [{K$_6$(OH$_2$)$_{12}$V$^{IV}_{11}$V$^V_7$O$_{41}$(PO$_4$)·4H$_2$O}$_n$] (**V$_{18}$P**) used in the biological experiments.

3.6. Aqueous solution stability of polyoxidovanadates with the {V$_{18}$O$_{42}$} shell

The analysis of $V_{18}P$ and $V_{18}I$ by ^{51}V NMR spectroscopy gave different results (Fig. 2). The spectra registered for $V_{18}I$ up to 1.0 mmol L^{-1} in water/D_2O (9:1) showed only one low-intensity signal at $\delta = -560$ ppm assigned to "V_1" ($H_2VO_4^-$) [56, 57], and no signal when higher concentrations were employed (5.0 and 10 mmol L^{-1}). Conversely, the spectra of $V_{18}P$ evidenced the breakdown of the polynuclear structure to produce a mixture of vanadium(V) species whose composition varied with sample concentration. In the most diluted solution (0.1 mmol L^{-1}), only a signal at $\delta = -560$ ppm assigned to "V_1" was observed. The spectral profile changed when the concentration was increased to 1.0 mmol L^{-1}, providing signals at $\delta = -556$, -572, and -576 ppm that correspond respectively to the rapid interconversion between "V_1' " (VO_2^+) and "V_1" (broadest line at -556 ppm), "V_2" ($H_2V_2O_7^{2-}$) and "V_4" ($V_4O_{12}^{4-}$) [56, 57]. At the highest concentrations (5.0 and 10 mmol L^{-1}), the signal produced by the "V_1' " $\Leftrightarrow$ "V_1" interconversion disappeared, revealing pure "VO_2^+" at -548 ppm along with an increase in the intensity of the "V_2", "V_4" and "V_5" ($V_5O_{15}^{5-}$) signals at $\delta = -569$, -576, and -584 ppm respectively [56, 57]. This profile evidences that $V_{18}P$ has a less stable structure in aqueous solution than $V_{18}I$, with a spectral pattern comparable to those observed in our previous work for the polyoxidovanadates $[V^{IV}_8V^V_7O_{36}Cl]^{6-}$ (V_{15}) [22] and $[H_6V^{IV}_2V^V_{12}O_{38}(PO_4)]^{5-}$ (V_{14}) [25].
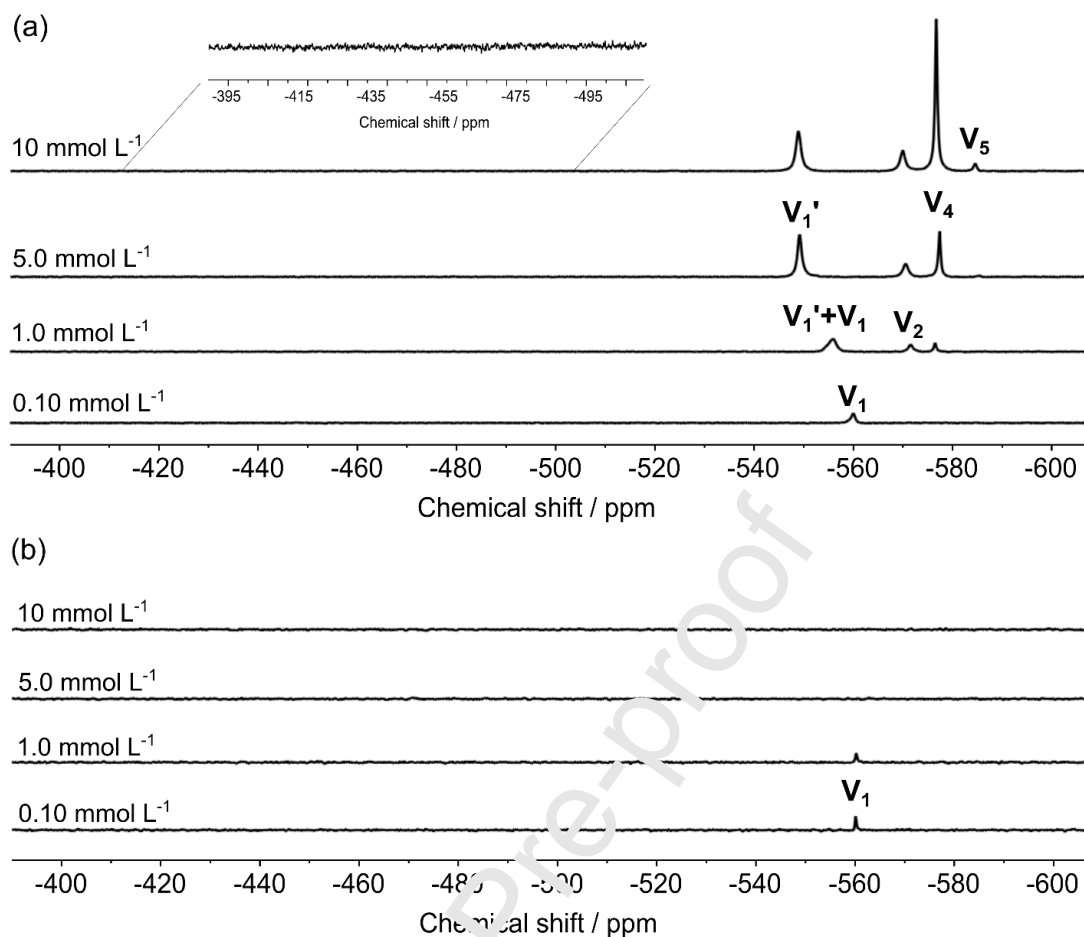
Fig. 2. [51]V NMR spectra recorded at room temperature for (a) $V_{18}P$ and (b) $V_{18}I$ in water/D_2O (9:1) solution at concentrations of 0.10 to 10 mmol L^{-1}. The measured pH was 5.0 for $V_{18}P$ solutions and 6.0 for $V_{18}I$. The insert in (a) shows a 10-fold amplification of the region from −390 to −525 ppm, to evidence the lack of any V_{10}-related signal. The low nuclearity vanadium(V) species identified in the spectra were "V_1'" = VO_2^+; "V_1" = $H_2VO_4^-$; "V_2" = $H_2V_2O_7^{2-}$; "V_4" = $V_4O_{12}^{4-}$; and "V_5" = $V_5O_{15}^{5-}$.

It is generally reported that aqueous vanadium(V) systems [58] present an equilibrium involving the fully-oxidized V_{10} species, $[V_{10}O_{28}]^{6-}$, and simple vanadates of lower nuclearity, while pure vanadium(IV) systems [58] show an equilibrium between cationic and anionic species, usually in a low pH range. Mixed-valence polyoxidovanadates, in turn, present even more complex equilibria in aqueous solution [59], as shown earlier for V_{15} and V_{14} [22, 25], and here for $V_{18}P$, containing mixtures of diamagnetic and paramagnetic species whose nature requires investigation by both [51]V NMR and EPR spectroscopies.

The solution EPR spectra of **V₁₈P** and **V₁₈I** were obtained in water at 77 K with increasing concentration of the products (0.10 to 10 mmol L^{-1}). For **V₁₈I** (Fig. 3), the presence of a broad signal in all concentrations evaluated, with a g value of 1.9674 and Δ_{p-p} of 33.13 mT, is characteristic of polynuclear species with magnetic interaction between the vanadium(IV) centers [60]. For **V₁₈P**, on the other hand, an analogous broad line (g = 1.9663 and Δ_{p-p} of 36.07 mT) overlaps a poorly resolved hyperfine signal of mononuclear vanadium(IV) species that likely results from a partial aggregate breakage (Fig. S9). This observation agrees with the results of the ^{51}V NMR analyses, which showed that **V₁₈P** is more susceptible than **V₁₈I** to decomposition in aqueous media.
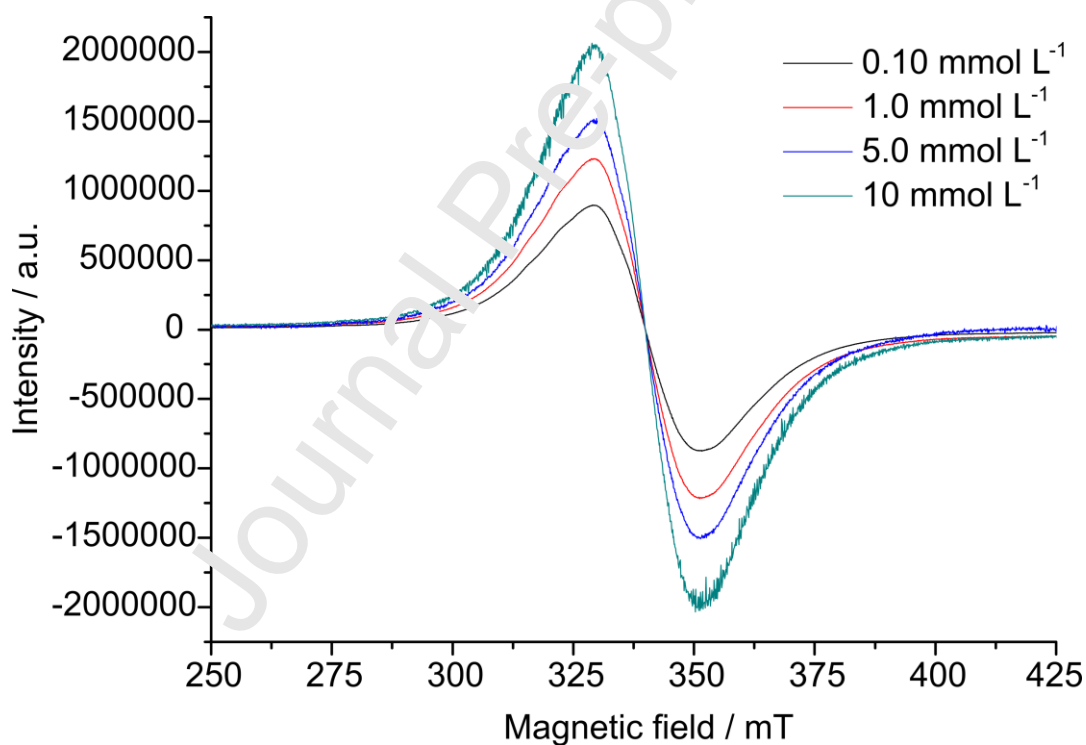
Fig. 3. X–band EPR spectra recorded at 77 K for aqueous solutions of **V₁₈I** in the concentration range of 0.10 to 10 mmol L^{-1}.

Recently, it was recognized that the charge, size, and shape of polyoxidovanadates have a fundamental role in the self-assembly, redox properties, and in the interaction of these polynuclear aggregates with biological targets [61, 62]. To the best of our knowledge, our current results with **V₁₈I** and **V₁₈P**, added to our previous findings [22, 25] with **V₁₅** and **V₁₄**

demonstrate, for the first time, that POVs containing encapsulated halides are more stable in aqueous solution than those containing the phosphate anion. The stability in aqueous medium seems to be a consequence not only of the size of the encapsulated anion but also of its charge, Cl^-/I^- *vs* PO_4^{3-}, to be accommodated by the spherical anionic "cage". The maintenance of the polynuclear structure, as observed for $V_{18}I$ and V_{15}, is rarely found in the literature; it has been reported for $[V_6O_8(OCH_3)_{11}]$ [63] and $[HV_{12}O_{32}Cl]^{4-}$ [64] but in both these cases the compounds are insoluble in water.

The mixed-valence character of $V_{18}I$ and $V_{18}P$ was also investigated in aqueous solution by UV/Vis/NIR spectroscopy (Fig. S10 and S11). Both absorption spectra showed a band with a maximum at 9900 cm^{-1} ($\varepsilon = 440$ L mol^{-1} cm^{-1}) attributed to an intervalence (V^{IV}/V^V) charge-transfer transition. The charge distribution in the products was classified as type II according to Robin–Day's criteria [65-67], which corresponds to partial delocalization of electrons in the polynuclear structure. Such classification was based on the analysis of theoretical and experimental values of the half-height bandwidth (Table S5). A similar classification was reported previously by our and other research groups for $[V^{IV}_8V^V_7O_{36}Cl]^{6-}$ [22], $[H_6V^{IV}_2V^V_{12}O_{38}(PO_4)]^{5-}$ [25] and $[V_{16}O_{38}(CN)]^{9-}$ [68].

3.7. The ability of polyoxidovanadates to act as chemoprotective agents against diethyl sulfate

The biological studies carried out in this work with $V_{18}P$ and $V_{18}I$ involved first the investigation of their toxicity towards *E. coli* cultures (Fig. 4a), and then the *in vitro* evaluation of their chemoprotective activity against the deleterious effect of diethyl sulfate (Fig. 4b) employing the same bacterial model. The chemoprotection results were compared with those obtained for decavanadate, $[\{Na_6(OH_2)_{20}V_{10}O_{28}\cdot 4H_2O\}_n]$ (V_{10}), which is the most common POV in acidic media, and for V_{15} [22].

The treatment of cultures with $V_{18}I$ (0.10 to 5.0 mmol L^{-1}) showed no significant difference in cell growth as compared with the control, indicating non-toxicity within these limits (Fig. 4a). At the lowest concentrations, this result was similar to the observed for V_{10}, but decavanadate was already toxic to *E. coli* DH5α cultures at 5.0 mmol L^{-1}. On the other hand, both $V_{18}I$ and V_{10} were lethal to cells at 10 mmol L^{-1}. Fig. 4a also shows that $V_{18}P$ is moderately cytotoxic to the cells in all concentrations accessed in this work. These results may be attributed to the nature of the chemical species formed by $V_{18}P$ in the aqueous medium (previous section) contrasted with the relatively higher stability of $V_{18}I$ in the same conditions.

Specifically for $V_{18}P$, because of the noticeable culture growth observed at the highest concentration (10 mmol L^{-1}), the experiment was repeated once more, and the results again confirmed the data. The only moderate cytotoxicity of $V_{18}P$ at 10 mmol L^{-1} is truly noteworthy, compared, at this point, to the results given by $V_{18}I$ and V_{10}. However, we have observed similar results for other polyoxidovanadates, for which there is a range of concentrations where a minor cytotoxicity is observed, and, above a certain threshold, an abrupt increase in cytotoxicity is seen. For instance, V_{14} showed such a steep toxicity increase above 5.0 mmol L^{-1}, while V_{15} was not toxic even at the highest concentration evaluated (10 mmol L^{-1}) [25].
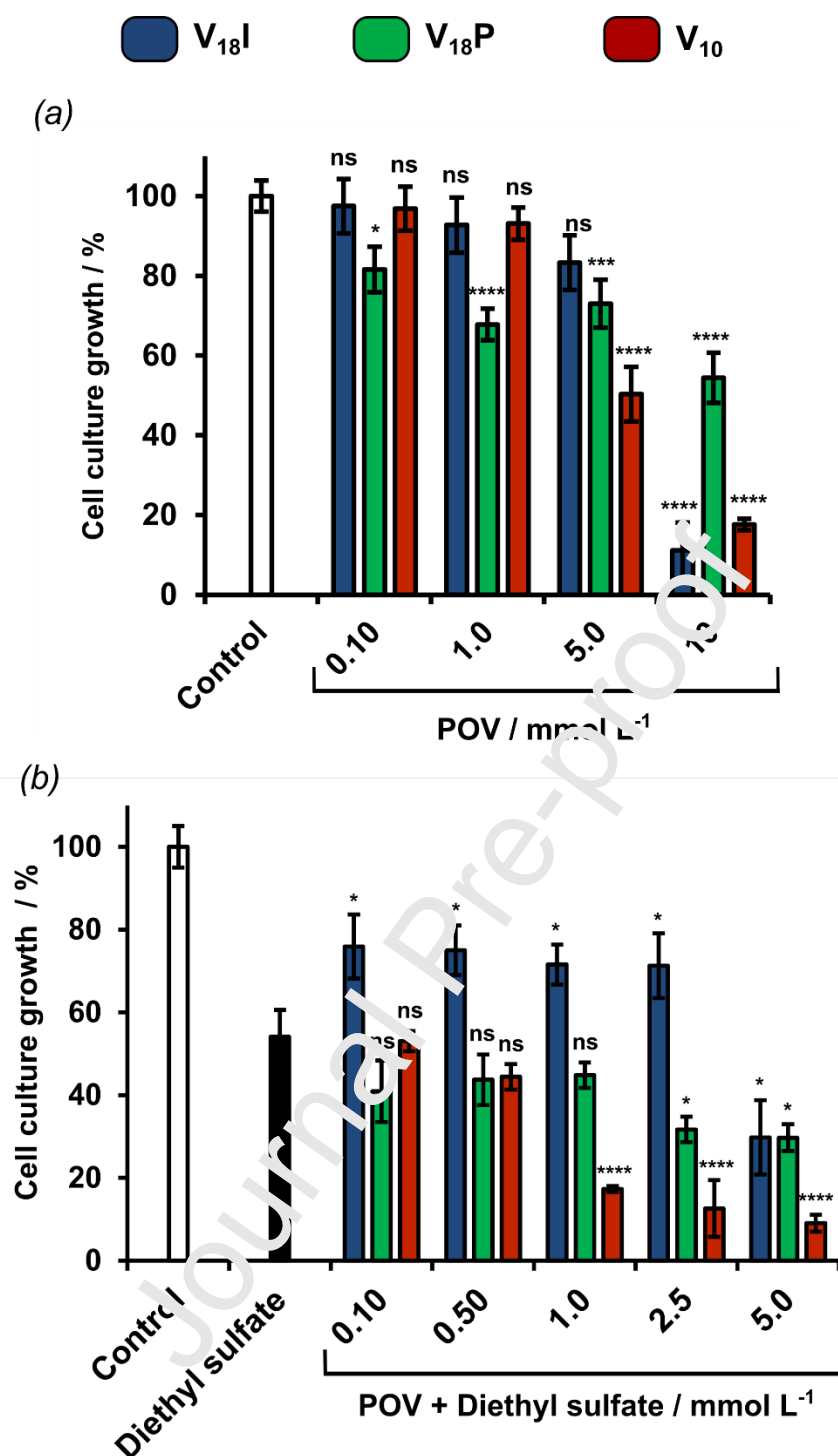
Fig. 4. Cell culture growth assays in *E. coli* suspensions treated with $V_{18}I$ (blue), $V_{18}P$ (green) and V_{10} (red) in concentrations from 0.10 to 10 mmol L^{-1}. *(a)* Toxicity assay, in which the OD_{595} value for the control (0.878±0.044) was considered 100% of growth. *(b)* Chemoprotection assay in the presence of 6.0 mmol L^{-1} of the alkylating agent diethyl sulfate. The OD_{595} value for the controls (0.878±0.044, 1.068±0.024, 0.742±0.043 for $V_{18}I$, $V_{18}P$ and V_{10}, respectively, without the addition of diethyl sulfate) were considered 100% of growth. Data were obtained in three independent experiments and results are given as average values with standard deviations. P-values, ANOVA corrected by Tukey, *P<0.01, ***P≤0.0001, ****P<0.0001, ns = non-significant when compared with the control in (a) and with the diethyl sulfate control in (b). A value of P < 0.05 was considered statistically significant.

$\mathbf{V_{10}}$ was recently described as a potential antibacterial agent, presenting GI$_{50}$ values from 0.58 to 1.8 mmol L^{-1} for different bacterial strains grown in similar conditions [69]. According to our previous research, this effect relates to a disbalance in the *E. coli* membrane potential that makes the cells permeable to toxic agents such as propidium iodide [6]. Additionally, $\mathbf{V_{10}}$ and the mixed-valence $\mathbf{V_{15}}$ were responsible for a decrease in membrane lipid packing in Chinese Hamster Ovary cells, initiating the signal transduction by the luteinizing hormone receptor (LHR) [70]. These findings point to a variety of effects of POVs on the cell membrane of different biological models and suggest that each POV, either intact or after breakage, acts differently towards cells when placed in physiological media.

For the chemoprotection assay, bacterial cells were first treated with $\mathbf{V_{18}I}$, $\mathbf{V_{18}P}$, and $\mathbf{V_{10}}$ (0.10 to 5.0 mmol L^{-1}) followed by addition of diethyl sulfate (6.0 mmol L^{-1}) and incubation for 3 h in LB medium. $\mathbf{V_{18}I}$ showed a significant positive effect of *ca.* 35% on bacterial growth, which was not concentration-dependent up to 2.5 mmol L^{-1} compared to the cells exposed only to diethyl sulfate (Fig. 4b). These results for $\mathbf{V_{18}I}$ were significantly different from both controls, without and with diethyl sulfate (Fig. S12), and confirm that the addition of diethyl sulfate is counteracted by the presence of $\mathbf{V_{18}I}$, although not completely, because the culture does not reach full growth in the presence of the alkylating agent. It is clear, though, that at 5.0 mmol L^{-1} the protective activity of $\mathbf{V_{18}I}$ is not only lost, but the deleterious effect of diethyl sulfate is even enhanced by the presence of the POV. In a related work, $\mathbf{V_{15}}$ presented a similar result (30–40% protection), and this again indicates that polynuclear frameworks that resist better to breakage in aqueous solution are also those more active towards diethyl sulfate to prevent an attack to the bacterial cells. The mechanism of such protective action by the (apparently) intact $\{V_nO_m\}^{y-}$ aggregates is still under investigation.

Additionally, electrostatic potential studies reported in the literature showed that the surface properties of V_{18} shells can change with the V^{IV}/V^{V} ratio; more negative electrostatic potentials at the surface, and therefore higher nucleophilicity, were registered for aggregates with higher negative charges [61]. In our case, considering that $[V^{IV}_{12}V^{V}_{6}O_{42}I]^{7-}$ (**$V_{18}I$**) has a higher charge density than $[V^{IV}_{11}V^{V}_{7}O_{41}(PO_4)]^{6-}$ (**$V_{18}P$**), this could increment its surface nucleophilicity and therefore its potential to act as a chemoprotective agent as opposed to **$V_{18}P$**. This agrees with both the mechanism proposed by Wilker and co-authors [23] and the results presented in this work. Moreover, the different growth levels shown in Fig. 4a and 4b reveal an increase in cytotoxicity when **$V_{18}P$** or **V_{10}** are mixed with diethyl sulfate, compared to cells treated only with the alkylating agent. This effect is more pronounced for **V_{10}** at and above 1.0 mmol L^{-1}. Additional essays should be performed to clarify if this enhanced toxic effect of **V_{10}** and **$V_{18}P$** in combination with diethyl sulfate is simply additive or synergistic, and if it could be explored further for antibacterial purposes.

3.8. Spectroscopic studies in POV solutions upon addition of diethyl sulfate

We also carried out speciation studies of **$V_{18}I$** and **$V_{18}P$** in LB broth to investigate the fate of the polymetallic aggregates in culture media after interaction with the alkylating agent and obtain additional insights on how the chemical nature of the vanadate could dictate its chemoprotective action. In these studies, we chose vanadium and diethyl sulfate proportions in the range of 1V:0(diethyl sulfate) to 1V:5(diethyl sulfate), to be comparable with the concentrations employed in our biological essays.

In the literature, the "carcinogen interception" mechanism, proposed from studies with pUC19 plasmid DNA as a model, suggests that the chemoprotective activity of polyoxidometalates involves the preferential transfer of alkyl groups from the alkylating agent to

the metal-containing aggregate, rather than to the DNA [22, 23]. This reaction eventually produces a new oxidometalate, deficient in one or more oxygen atoms, and alcohol molecules (ROH, with R depending on the alkylating agent) that are less toxic to the cells. The following equations apply this proposal to the mixed valence polynuclear systems described in this work. The vanadium-containing species in each equation are based on the results of our ^{51}V NMR and EPR studies in solution, both aqueous (already discussed) and in LB (see below), and therefore involve both diamagnetic and paramagnetic compounds.

$$\mathbf{V_{18}I}$$

$$\text{MV-POV} + \text{V}^{IV}\text{O}^{2+} + [\text{C}_2\text{H}_5]^{\bullet} \overset{\text{LB}}{\rightarrow} \text{MV-POV}^{'} + \text{V}^{IV}\text{O}(\text{L}) + \text{C}_2\text{H}_5\text{OH}$$

$$\mathbf{V_{18}P}$$

$$\text{MV-POV} + \text{V}^{IV}\text{O}^{2+} + \text{V}_1^{'} + \text{V}_2 + \text{V}_4 + [\text{C}_2\text{H}_5]^{\bullet}$$
$$\overset{\text{LB}}{\rightarrow} \text{MV-POV}^{'} + \text{V}_1 + \text{PV} + \text{V}_2^{'} + \text{V}_4 + \text{V}^{IV}\text{O}(\text{L}) + \text{C}_2\text{H}_5\text{OH}$$
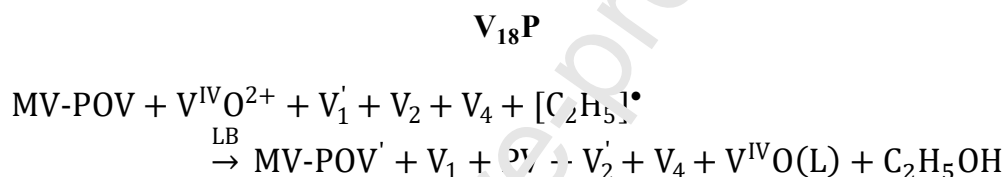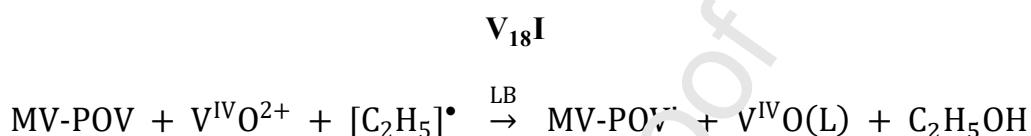
$\text{V}^{IV}\text{O}(\text{L})$ = product formed from the V^{IV} species released from the breakage of the POV and potential ligands in LB buffer; $\text{V}_1 = \text{H}_2\text{VO}_4^-$; "$\text{V}_1^{'}$" = VO_2^-; PV = HVPO_7^{3-}; $\text{V}_2 = \text{H}_2\text{V}_2\text{O}_7^{2-}$; "$\text{V}_2^{'}$" = $\text{HV}_2\text{O}_7^{3-}$; V_4 = $\text{V}_4\text{O}_{12}^{4-}$; $[\text{C}_2\text{H}_5]^{\bullet}$: alkyl group provided by diethyl sulphate.

Interestingly, the ^{51}V NMR spectra of **V$_{18}$I** in LB medium with increasing concentrations of diethyl sulfate did not show any signal of low-nuclearity vanadium(V) species (Fig. 5); this is consistent with the behavior observed in pure aqueous solutions. For **V$_{18}$P**, on the other hand, the ^{51}V NMR results are close to those reported for **V$_{14}$** and **V$_{15}$** (Table 2) [22, 25]. The spectra of **V$_{18}$P** up to the 1V:0.10(diethyl sulfate) proportion show the formation and consecutive consumption of low nuclearity species: "V_1+PV" [71], which is the signal generated by the rapid equilibrium between "V_1" (H_2VO_4^-) and a vanadium complex with phosphate (PV = HVPO_7^{3-}) [57], "V_2" ($\text{H}_2\text{V}_2\text{O}_7^{2-}$) and "$\text{V}_4$" ($\text{V}_4\text{O}_{12}^{4-}$). However, there is no evidence of additional breakage of the polynuclear structure when a high concentration of diethyl sulfate is employed. Our observations agree with reactivity studies described in the literature for acetonitrile solutions, in which oligovanadates such as $[\text{V}_3\text{O}_9]^{3-}$, $[\text{HV}_4\text{O}_{12}]^{4-}$, and $[\text{V}_5\text{O}_{14}]^{3-}$ were shown to react with

diethyl sulfate to form rearranged products [23]. In this context, it was reported that any oxygen-deficient POM derivative formed by an oxide reaction with the alkyl group of diethyl sulfate can further rearrange in one or more new polynuclear aggregates [23, 24].
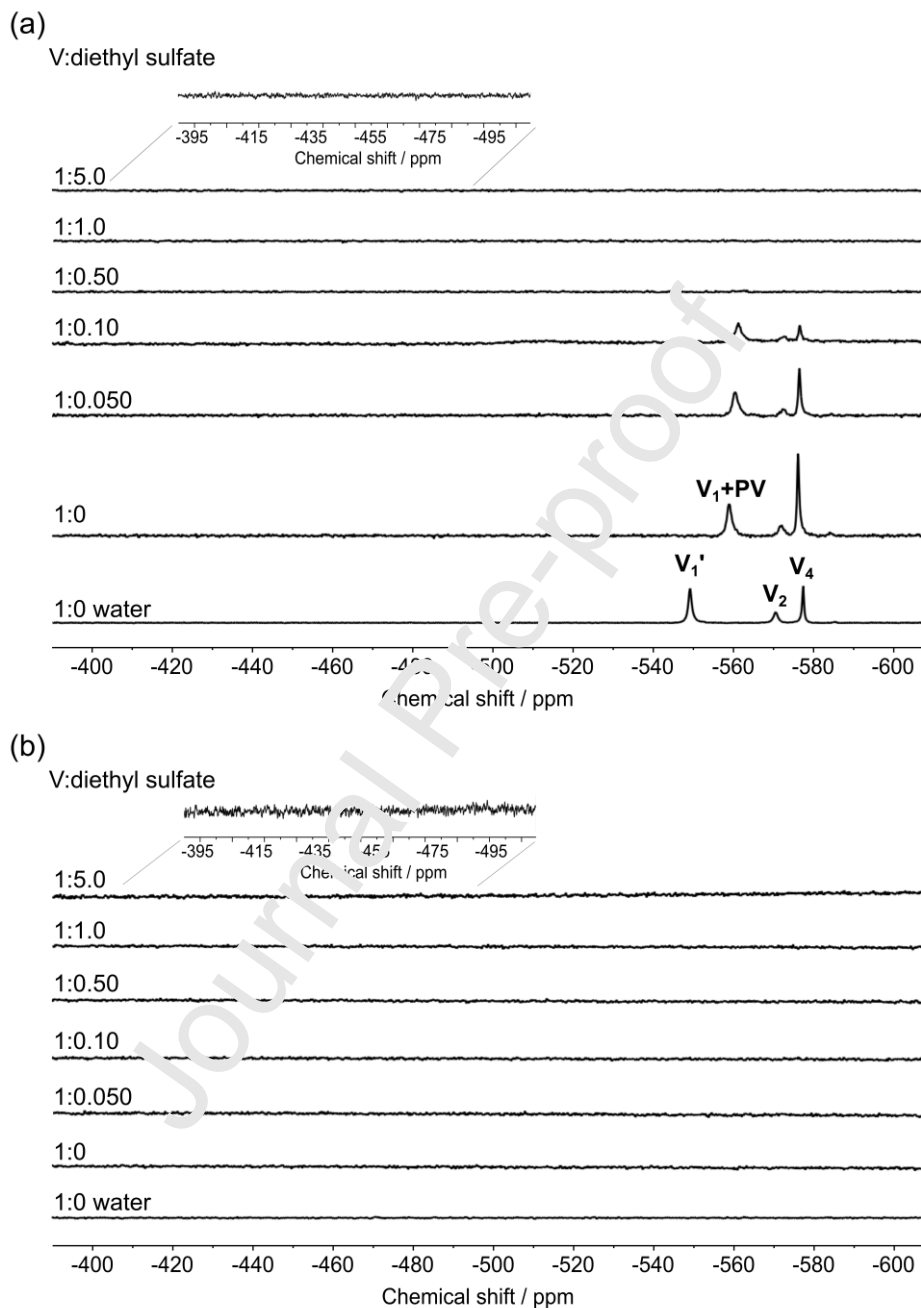
Fig. 5. ^{51}V NMR spectra recorded for (a) **V$_{18}$P** and (b) **V$_{18}$I** in LB medium pH 6.0 (5.0 mmol L^{-1}) with increasing concentrations of the alkylating agent (diethyl sulfate). The V:diethyl sulfate proportions are indicated in the figure. For comparison, the spectra recorded for both polyoxidovanadates (5.0 mmol L^{-1}) in water / D$_2$O (9:1) are also presented at the bottom of each set of spectra. The solution pH varied with the addition of diethyl sulfate from 6.0 to 4.5 for **V$_{18}$P** and 6.0 to 5.0 with **V$_{18}$I**. The inserts in (a) and (b) show a 10-fold amplification of the region from –390 to –525 ppm, to evidence the lack of any V$_{10}$-related signal. The low nuclearity vanadium(V) species identified in the spectra were "V$_1$' " = VO$_2^+$; "V$_1$" = H$_2$VO$_4^-$; "V$_2$" = H$_2$V$_2$O$_7^{2-}$; "V$_4$" = V$_4$O$_{12}^{4-}$; and "PV" = HVPO$_7^{3-}$.

Table 2 The proposed composition of the **V$_{18}$I**, **V$_{18}$P**, **V$_{14}$** [25], and **V$_{15}$** [22] aqueous and LB solutions starting from a concentration of 5.0 mmol L^{-1} of the MV-POV (*)

Product	pH[a]	V^{V} species[b]	V^{IV} species[c]	V^{V} species[b]	V^{IV} species[c]
		Aqueous solution		LB solution	
V$_{18}$I	6.0	None	MV-POV[d]	None	MV-POV, VO(L)
V$_{18}$P	5.0	V$_1$', V$_2$, V$_4$	MV-POV, VO^{2+}	PV, V$_1$', V$_2$, V$_4$	MV-POV, VO(L)
V$_{15}$	6.3	V$_1$, V$_2$, V$_4$, V$_5$	MV-POV, VO^{2+}	PV, V$_1$	MV-POV, VO(L)
V$_{14}$	4.2	V$_{14}$', V$_{10}$	MV-POV	V$_{10}$	MV-POV, VO(L)
NaV$_{10}$	4.0	V$_{10}$	None	V$_{10}$, PV, V$_1$	None

(*) This table summarizes the NMR and EPR results presented in this and the following sections of this work. Please see the text for discussion.
(a) pH obtained after solubilization in water except for **NaV$_{10}$**, in which solution the pH was adjusted. (b) Determined by ^{51}V NMR. (c) Determined by X-band EPR. (d) MV-POV = mixed-valence polyoxidovanadate. VO(L) = product formed from the V^{IV} species released from the breakage of the POV and potential ligands in the LB buffer. The low nuclearity vanadium(V) species mentioned are "V$_1$'" = VO$_2^+$; "V$_1$" = H$_2$VO$_4^-$; "V$_2$" = H$_2$V$_2$O$_7^{2-}$; "PV" = HVPO$_7^{3-}$; "V$_{14}$'" = H$_4$V$_{14}$O$_{42}$P^{5-}.

Our results also indicate that, if a direct reaction occurs between the polyoxidovanadates and the alkylating agent, it does not produce (in the time scale of the NMR analysis) small-nuclearity vanadium(V) species as final products. This is because such diamagnetic molecules would be detectable by ^{51}V NMR, differently from paramagnetic, mixed-valence polynuclear species. By contrast, we have shown that, in similar conditions, **V$_{14}$** [25] and **V$_{15}$** [22] undergo breakage and form the more stable decavanadate(V), **V$_{10}$**, anion. Interestingly, the formation of **V$_{10}$** was not observed in either **V$_{18}$P** or **V$_{18}$I** solutions. We also made attempts to react **V$_{10}$** with diethyl sulfate in the same experimental conditions employed for **V$_{18}$P** and **V$_{18}$I** (Fig. S13). The spectrum presents signals assigned to H$_2$V$_{10}$O$_{28}^{4-}$ and V$_4$ up to the 1V:0.10(diethyl sulfate) proportion. Our results also show changes in the protonation degree of **V$_{10}$**, which goes from H$_2$V$_{10}$O$_{28}^{4-}$ to H$_4$V$_{10}$O$_{28}^{2-}$. In the highest concentration of diethyl sulfate, H$_4$V$_{10}$O$_{28}^{2-}$ suffers a partial hydrolysis (forming a small amount of V$_1$') usually observed in acidic solutions of decavanadate (Fig. S13) [57]. These results agree with earlier reports that describe decavanadate as a relatively poor reactant in contact with diethyl sulfate in acetonitrile [23].

The EPR spectra of **V₁₈I** and **V₁₈P** in LB medium, registered in the same conditions of the ^{51}V NMR analyses, present a quite different pattern compared to the spectra recorded from aqueous solutions. As seen in Fig. 6, they present a typical hyperfine pattern of a mononuclear species superimposed to the broad line of the polynuclear components. For both MV-POV, the g values and the Δ_{p-p} are the same in aqueous and LB media, indicating that the chemical nature of the polynuclear species is maintained in LB. On the other hand, the spectral simulation of the mononuclear components provide EPR parameters (Table S6) that are mostly the same for **V₁₈I** and **V₁₈P** and differ from the parameters reported for $[V^{IV}O(OH_2)_5]^{2+}$, "VO^{2+}", the usual vanadyl(IV) species formed in aqueous solution. This suggests that a new mononuclear species, $V^{IV}O(L)$, might be formed by the interaction of the vanadium ions with components of the LB medium (Fig. 6a and 6c).
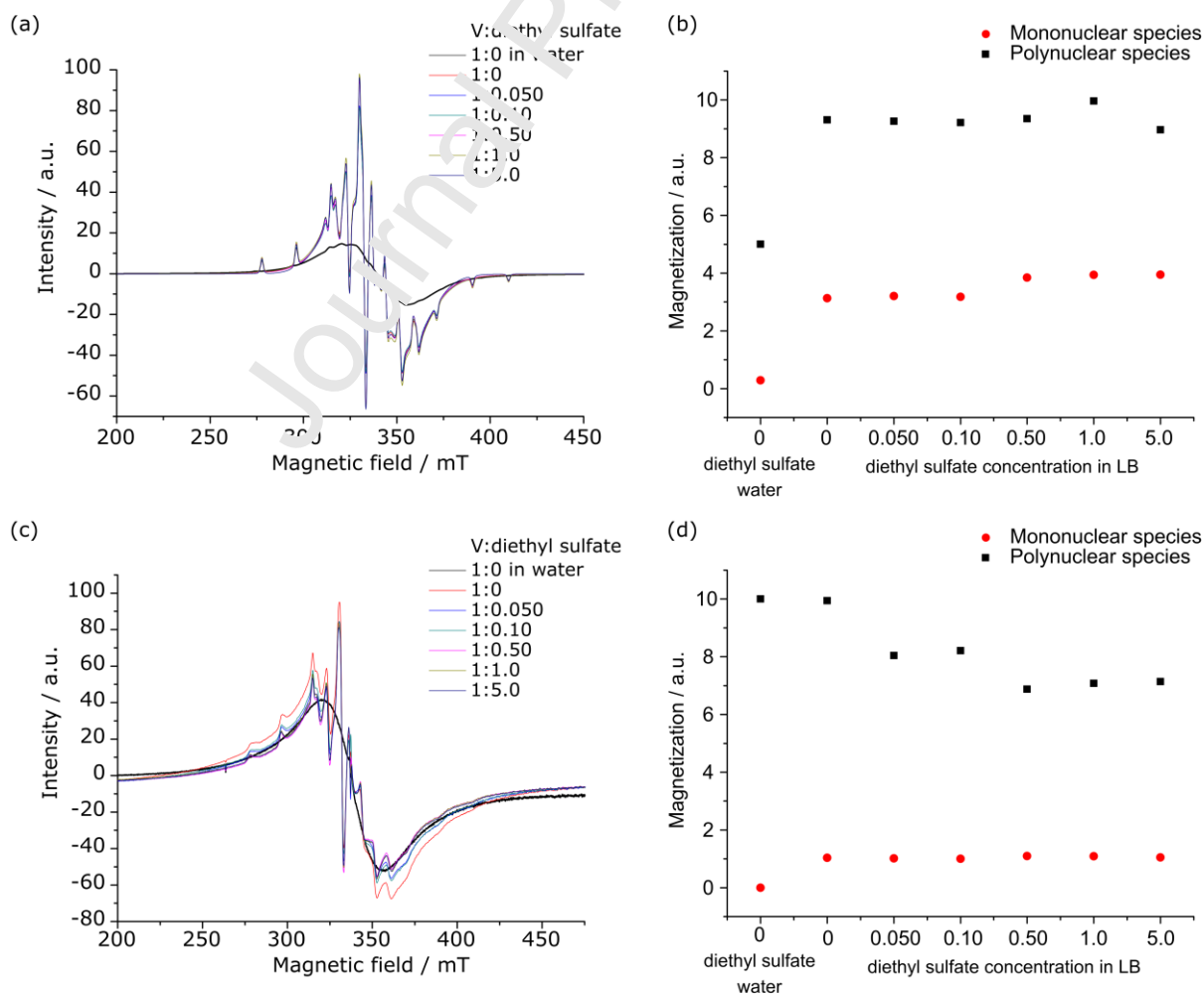
Fig. 6. X–band EPR spectra recorded at 77 K, in the presence of a MgO/Cr^{3+} marker, for 5.0 mmol L^{-1} solutions of *(a)* **V$_{18}$I** and *(c)* **V$_{18}$P** in water and LB with increasing proportions of diethyl sulfate. The contribution of the mononuclear and polynuclear components for the total magnetization of the systems (estimated by simulation and integration of the signals given by the different species for a fixed amount of vanadium) are shown in *(b)* and *(d)* for increasing concentrations of diethyl sulfate. Please note that both the plots *(b)* and *(d)* show the results obtained in pure aqueous solutions (as the first entry in each graphic) for comparison.

The relative contributions of the mononuclear and polynuclear species to the total magnetization of **V$_{18}$I** and **V$_{18}$P** in aqueous and LB solutions were estimated by spectral simulation/integration and are presented in Fig. 6b and 6d. Subtle differences were observed for **V$_{18}$I** with increasing concentration of diethyl sulfate, suggesting, once more, a higher solution stability of this aggregate. This finding agrees with the results of theoretical calculations carried out for an analogous [V$_{18}$O$_{42}$I]$^{5-}$ anion, which suggests an association of POVs in solution, assisted by the counterions [72], contributing to the maintenance of the polynuclear structure.

V$_{18}$P, in turn, revealed once again to be a more dynamic system, with a varying contribution of the polynuclear component following addition of different amounts of diethyl sulfate. This variation possibly comes from the formation of a rearranged polynuclear species from the original **V$_{18}$P** after reaction with diethyl sulfate, which can also explain the lack of ^{51}V NMR signals above the 1V:0.1(diethyl sulfate) proportion in Fig. 6a. All these results, taken together, suggest that the chemoprotective effect (or its absence) is not only related to the maintenance of the original polynuclear structure in the culture medium, but also to a delicate equilibrium involving non-toxic species.

In summary, the effect of the encapsulated anion on the POV-stability in aqueous and LB media was studied in this work and correlated with our previous results on other polynuclear aggregates (Fig. 7). **V$_{18}$I** proved to be more stable than **V$_{15}$**, followed by **V$_{18}$P** and **V$_{14}$**, and this stability appears to be decisive in their interaction with cells and their chemoprotective action against the deleterious effect of diethyl sulfate [73-77]. Both ^{51}V NMR and EPR results evidence

maintenance of the MV-POV structure in the same chemical systems where the highest chemoprotection activity was detected (Fig. 7), that is, the halide-containing polyoxidoanions $V_{18}I$ and V_{15}.
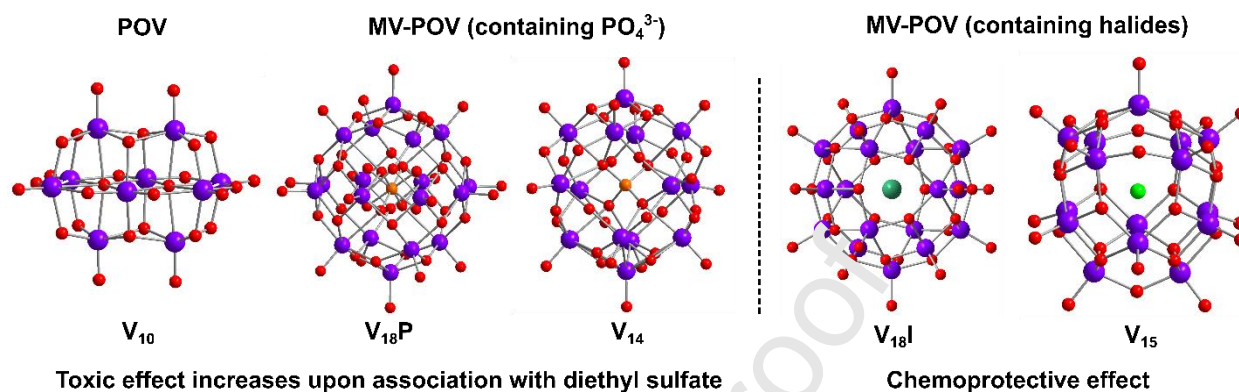
Fig. 7. Ball-and-stick representations of the polyoxidoanions $[V^V_{10}O_{28}]^{6-}$ (V_{10}), $[V^{IV}_{11}V^V_7O_{41}(PO_4)]^{6-}$ ($V_{18}P$), $[H_6V^{IV}_2V^V_{12}O_{38}(PO_4)]^{5-}$ (V_{14}), $[V^{IV}_{12}V^V_6O_{42}I]^{7-}$ ($V_{18}I$) and $[V^{IV}_8V^V_7O_{36}Cl]^{6-}$ (V_{15}). The hydrogen atoms and counterions were omitted for clarity. The polyoxidoanions were grouped according to the biological effect and associated stability in the LB media. Vanadium atoms are shown in purple, oxygen in red, phosphorus in orange, iodine in green, and chlorine in light green.

4. Conclusions

The methodology adopted in this work was efficient for the preparation of two variants of pseudospherical mixed valence octadecavanadates, $\{V_{18}O_{42}X\}$, containing encapsulated phosphate ($V_{18}P$) and iodide ($V_{18}I$) anions, and rationally expanded the accessible route that we described earlier for the preparation of this class of polymetallic aggregates [22, 25]. The choice of anion to be encapsulated, the nature of the organic reducing agent, the pH, and the reaction temperature were crucial variables in the rational synthesis of each POV.

This work brings new insights into the reactivity of polyoxidovanadates towards diethyl sulfate and investigates further the chemoprotective activity of $V_{18}I$, $V_{18}P$, and decavanadate (V_{10}) anions using *E. coli* as a biological model. The results can be interpreted in the light of the hypothesis raised by Wilker and co-workers [23, 24] of a DNA-protection mechanism involving

the preferential transfer of the alkyl group from the alkylating agent to the vanadium-containing species, rather than to the DNA. The chemoprotective activity of each POV apparently correlates to its stability in the biological medium and to the generation of other vanadium species that are less toxic and/or more nucleophilic towards diethyl sulfate. Regarding these two key features, $V_{18}I$ and the previously described V_{15} [22] seem to be the most promising polyanions because they provide the best structural stability-activity relationship, and therefore deserve in-depth studies aiming at the design of more effective and selective candidates for the therapeutic use of vanadium compounds.

Declaration of competing interest

The authors declare that they have no known competing financial interests or personal relationships that could have appeared to influence the work reported in this paper.

Acknowledgments

Author statement

Kahoana Postal: Investigation (Synthesis and Biological assays); Francielli S. Santana: Crystallographic Analysis; David L. Hughes: Crystallographic Analysis; André L. Rüdiger:

Investigation (^{51}V NMR analysis); Ronny R. Ribeiro, Investigation (EPR analysis); Eduardo L. Sá: validation; Emanuel M. de Souza: Supervision (Biological assays); Jaísa F. Soares: Conceptualization, Supervision; Giovana G. Nunes: Conceptualization, Supervision.

Appendix A. Supplementary data

Supplementary data to this article can be found online at http://xxxxxxxxxx.

CCDC: 2022169 can be obtained at http://www.ccdc.cam.ac.uk/structures.

References

[1] M.S. Bhuiyan, K. Fukunaga, Cardioprotection by vanadium compounds targeting Akt-mediated signaling, *Journal of Pharmacological Sciences*, **2009**, 110, 1-13. DOI: 10.1254/jphs.09r01cr

[2] S. Treviño, D. Velázquez-Vázquez, E. Sánchez-Lara, A. Diaz-Fonseca, J.Á. Flores-Hernandez, A. Pérez-Benítez, E. Brambila-Colombres, E. González-Vergara, Metforminium Decavanadate as a Potential Metallopharmaceutical Drug for the Treatment of Diabetes Mellitus, *Oxidative Medicine and Cellular Longevity*, **2016**, 2016, 6058705-6058705. DOI: 10.1155/2016/6058705

[3] A. Ścibior, Ł. Pietrzyk, Z. Plewa, A. Skiba, Vanadium: Risks and possible benefits in the light of a comprehensive overview of its pharmacotoxicological mechanisms and multi-applications with a summary of further research trends, *Journal of Trace Elements in Medicine and Biology*, **2020**, 61, 126508. DOI: 10.1016/j.jtemb.2020.126508

[4] A. Bijelic, M. Aureliano, A. Rompel, The antibacterial activity of polyoxometalates: structures, antibiotic effects and future perspectives, *Chemical Communications*, **2018**, 54, 1153-1169. DOI: 10.1039/C7CC07549A

[5] D. Rehder, The potentiality of vanadium in medicinal applications, *Inorganica Chimica Acta*, **2020**, 504, 119445. DOI: 10.1016/j.ica.2020.119445

[6] J.M. Missina, B. Gavinho, K. Postal, F.S. Santana, G. Valdameri, E.M. de Souza, D.L. Hughes, M.I. Ramirez, J.F. Soares, G.G. Nunes, Effects of Decavanadate Salts with Organic and Inorganic Cations on Escherichia coli, Giardia intestinalis, and Vero Cells, *Inorganic Chemistry*, **2018**, 57, 11930-11941. DOI: 10.1021/acs.inorgchem.8b01298

[7] D. Gambino, Potentiality of vanadium compounds as anti-parasitic agents, *Coordination Chemistry Reviews*, **2011**, 255, 2193-2203. DOI: 10.1016/j.ccr.2010.12.028

[8] M. Pisano, C. Arru, M. Serra, G. Galleri, D. Sanna, E. Garribba, G. Palmieri, C. Rozzo, Antiproliferative activity of vanadium compounds: effects on the major malignant melanoma molecular pathways, *Metallomics*, **2019**, 11, 1687-1699. DOI: 10.1039/C9MT00174C

[9] A. Bijelic, M. Aureliano, A. Rompel, Polyoxometalates as Potential Next-Generation Metallodrugs in the Combat Against Cancer, *Angewandte Chemie International Edition* **2019**, 58, 2980-2999. DOI: 10.1002/anie.201803868

[10] M. Selman, C. Rousso, A. Bergeron, H.H. Son, R. Krishnan, N.A. El-Sayes, O. Varette, A. Chen, F. Le Boeuf, F. Tzelepis, J.C. Bell, D.C. Crans, J.S. Diallo, Multi-modal Potentiation of Oncolytic Virotherapy by Vanadium Compounds, *Molecular Therapy: The Journal of the American Society of Gene Therapy*, **2018**, 26, 56-69. DOI: 10.1016/j.ymthe.2017.10.014

[11] A. Ross, D.C. Soares, D. Covelli, C. Pannecouque, L. Budd, A. Collins, N. Robertson, S. Parsons, E. De Clercq, P. Kennepohl, P.J. Sadler, Oxovanadium(IV) Cyclam and Bicyclam Complexes: Potential CXCR4 Receptor Antagonists, *Inorganic Chemistry*, **2010**, 49, 1122-1132. DOI: 10.1021/ic9020614

[12] F. Renata, M. Krosniak, M. Barlik, A. Kudła, R. Grybos, T. Librowski, Impact of Vanadium Complexes Treatment on the Oxidative Stress Factors in Wistar Rats Plasma, *Bioinorganic Chemistry and Applications*, **2011**, 2011, 206316. DOI: 10.1155/2011/206316

[13] X. Liao, J. Lu, P. Ying, P. Zhao, Y. Bai, W. Li, M. Liu, DNA binding, antitumor activities, and hydroxyl radical scavenging properties of novel oxovanadium(IV) complexes with substituted isoniazid, *Journal of Biological Inorganic Chemistry*, **2013**, 18, 975-984. DOI: 10.1007/s00775-013-1046-9

[14] A.M. Evangelou, Vanadium in cancer treatment, *Critical Reviews in Oncology/Hematology*, **2002**, 42, 249-265. DOI: 10.1016/S1040-8428(01)00221-9

[15] A. Bishayee, R. Karmakar, A. Mandal, S.N. Kundu, M. Chatterjee, Vanadium-mediated chemoprotection against chemical hepatocarcinogenesis in rats: haematological and histological characteristics, *European Journal of Cancer Prevention: The Official Journal of the European Cancer Prevention Organisation*, **1997**, 6, 58-70. DOI: 10.1097/00008469-199702000-00010

[16] S. Samanta, V. Swamy, D. Suresh, M. Rajkumar, B. Rana, A. Rana, M. Chatterjee, Protective effects of vanadium against DMH-induced genotoxicity and carcinogenesis in rat colon: removal of O(6)-methylguanine DNA adducts, p53 expression, inducible nitric oxide synthase downregulation and apoptotic induction, *Mutation Research*, **2008**, 650, 123-131. DOI: 10.1016/j.mrgentox.2007.11.001

[17] T. Chakraborty, A. Chatterjee, A. Rana, D. Dhachinamoorthi, A. Kumar P, M. Chatterjee, Carcinogen-induced early molecular events and its implication in the initiation of chemical hepatocarcinogenesis in rats: Chemopreventive role of vanadium on this process, *Biochimica et Biophysica Acta - Molecular Basis of Disease*, **2007**, 1772, 48-59. DOI: 10.1016/j.bbadis.2006.10.019

[18] A. Bishayee, A. Waghray, M.A. Patel, M. Chatterjee, Vanadium in the detection, prevention and treatment of cancer: The in vivo evidence, *Cancer Letters*, **2010**, 294, 1-12. DOI: 10.1016/j.canlet.2010.01.030

[19] A. Basu, A. Bhattacharjee, S.S. Roy, P. Ghosh, P. Chakraborty, I. Das, S. Bhattacharya, Vanadium as a chemoprotectant: effect of vanadium(III)-l-cysteine complex against cyclophosphamide-induced hepatotoxicity and genotoxicity in Swiss albino mice, *Journal of Biological Inorganic Chemistry*, **2014**, 19, 981-996. DOI: 10.1007/s00775-014-1141-6

[20] A. Basu, A. Bhattacharjee, S. Hajra, A. Samanta, S. Bhattacharya, Ameliorative effect of an oxovanadium (IV) complex against oxidative stress and nephrotoxicity induced by cisplatin, *Redox Report*, **2017**, 22, 377-387. DOI: 10.1080/13510002.2016.1260192

[21] E.E. Hamilton, J.J. Wilker, Inhibition of DNA alkylation damage with inorganic salts, *Journal of Biological Inorganic Chemistry*, **2004**, 9, 894-902. DOI: 10.1007/s00775-004-0597-1

[22] G.G. Nunes, A.C. Bonatto, C.G. de Albuquerque, A. Barison, R.R. Ribeiro, D.F. Back, A.V.C. Andrade, E.L. de Sá, F.d.O. Pedrosa, J.F. Soares, E.M. de Souza, Synthesis, characterization and chemoprotective activity of polyoxovanadates against DNA alkylation, *Journal of Inorganic Biochemistry*, **2012**, 108, 36-46. DOI: 10.1016/j.jinorgbio.2011.11.019

[23] E.E. Hamilton, P.E. Fanwick, J.J. Wilker, Alkylation of Inorganic Oxo Compounds and Insights on Preventing DNA Damage, *Journal of the American Chemical Society*, **2006**, 128, 3388-3395. DOI: 10.1021/ja056568v

[24] E.E. Hamilton, J.J. Wilker, Inorganic Oxo Compounds React with Alkylating Agents: Implications for DNA Damage, *Angewandte Chemie International Edition*, **2004**, 43, 3290-3292. DOI: 10.1002/anie.200353363

[25] K. Postal, D.F. Maluf, G. Valdameri, A.L. Rudiger, D.L. Hughes, E.L.d. Sa, R.R. Ribeiro, E.M.d. Souza, J. Fernandes Soares, G.G. Nunes, Chemoprotective activity of mixed valence polyoxovanadates against diethylsulfate in E. coli cultures: insights from chemichal speciation studies, *RSC Advances*, **2016**, 115, 114955-114968. DOI: 10.1039/C6RA15826A

[26] A. Müller, R. Sessoli, E. Krickemeyer, H. Bögge, J. Meyer, D. Gatteschi, L. Pardi, J. Westphal, K. Hovemeier, R. Rohlfing, J. Döring, F. Hellweg, C. Beugholt, M. Schmidtmann, Polyoxovanadates: High-Nuclearity Spin Clusters with Interesting Host−Guest Systems and Different Electron Populations. Synthesis, Spin Organization, Magnetochemistry, and Spectroscopic Studies, *Inorganic Chemistry*, **1997**, 36, 5239-5250. DOI: 10.1021/ic9703641

[27] A. Wutkowski, F. Niefind, C. Näther, W. Bensch, A New Mixed-Valent High Nuclearity Polyoxovanadate Cluster Based on the $\{V_{18}O_{42}\}$ Archetype, *Zeitschrift für Anorganische und Allgemeine Chemie*, **2011**, 637, 2198-2204. DOI: 10.1002/zaac.201100329

[28] S. Mulkapuri, S.K. Kurapati, S.K. Das, Carbonate encapsulation from dissolved atmospheric CO_2 into a polyoxovanadate capsule, *Dalton Transactions*, **2019**, 48, 8773-8781. DOI: 10.1039/C9DT01103J

[29] M.I. Khan, E. Yohannes, R.J. Doedens, $[M_3V_{18}O_{42}(H_2O)_{12}(XO_4)]\cdot 24\,H_2O$ (M=Fe, Co; X=V, S): Metal Oxide Based Framework Materials Composed of Polyoxovanadate Clusters, *Angewandte Chemie International Edition*, **1999**, 38, 1292-1294. DOI: 10.1002/(SICI)1521-3773(19990503)38:9<1292::AID-ANIE1292>3.0.CO;2-2

[30] T. Yamase, M. Suzuki, K. Ohtaka, Structures of photochemically prepared mixed-valence polyoxovanadate clusters. oblong $[V_{18}O_{44}(N_3)]^{14-}$, superkeggin $[V_{18}O_{42}(PO_4)]^{11-}$ and doughnut-shaped $[V_{12}B_{32}O_{84}Na_4]^{15-}$ anions, *Journal of the Chemical Society, Dalton Transactions*, **1997**, 2463-2472. DOI: 10.1039/A700916J

[31] L. Wang, H. Fan, C. Du, X. Xing, Y. Zhao, B. Chen, L. Wang, Synthesis, structure and properties of a Co-crystallized complex based on polyoxovanadate $[V^{IV}_{12}V^{V}_{6}O_{42}]^{6-}$ and a mononuclear vanadium complex $[VON(CH_2CH_2O)_3]$, *Inorganic Chemistry Communications*, **2016**, 63, 39-41. DOI: 10.1016/j.inoche.2015.11.011

[32] X.-M. Lin, X.-D. Feng, Y. Wang, Y.-H. Xing, L.-X. Sun, S.-Y. Wei, Z. Shi, Polyoxidovanadate complexes: synthesis, structures and catalytic oxidative bromination of phenol red, *Journal of Coordination Chemistry*, **2017**, 70, 44-59. DOI: 10.1080/00958972.2016.1247445

[33] Y.-Y. Zhou, S. Yao, J.-H. Yan, L. Chen, T.-T. Wang, C.-J. Wang, Z.-M. Zhang, Design and synthesis of purely inorganic 3D frameworks composed of reduced vanadium clusters and manganese linkers, *Dalton Transactions*, **2015**, 44, 20435-20440. DOI: 10.1039/C5DT03397G

[34] W. Qi, B. Zhang, Y. Qi, S. Guo, R. Tian, J. Sun, M. Zhao, The Anti-Proliferation Activity and Mechanism of Action of $K_{12}[V_{18}O_{42}(H_2O)]\cdot 6H_2O$ on Breast Cancer Cell Lines, *Molecules*, **2017**, 22, 1535. DOI: 10.3390/molecules22091535

[35] L. Roubatis, N.C. Anastasiadis, C. Paratriantafyllopoulou, E. Moushi, A.J. Tasiopoulos, S.C. Karkabounas, P.G. Veltsistas, S.P. Perlepes, A.M. Evangelou, A missing oxidation-state level in the family of polyoxo(azide)octadecavanadate(IV/V) clusters: Synthesis, structure and antitumoural properties of $[V^{IV}_{11}V^{V}_{7}O_{44}(N_3)]^{10-}$ in a sodium containing-3D architecture, *Inorganic Chemistry Communications*, **2016**, 69, 85-88. DOI: 10.1016/j.inoche.2016.04.019

[36] E. Kioseoglou, S. Petanidis, C. Gabriel, A. Salifoglou, The chemistry and biology of vanadium compounds in cancer therapeutics, *Coordination Chemistry Reviews*, **2015**, 301. DOI: 10.1016/j.ccr.2015.03.010

[37] S. Yerra, B.K. Tripuramallu, S.K. Das, Decavanadate-based discrete compound and coordination polymer: Synthesis, crystal structures, spectroscopy and nano-materials, *Polyhedron*, **2014**, 81, 147-153. DOI: 10.1016/j.poly.2014.05.035

[38] J. Woolcock, A. Zafar, Microscale techniques for determination of magnetic susceptibility, *Journal of Chemical Education*, **1992**, 69, A176. DOI: 10.1021/ed069pA176

[39] Z.S. Teweldemedhin, R.L. Fuller, M. Greenblatt, Magnetic Susceptibility Measurements of Solid Manganese Compounds with Evan's Balance, *Journal of Chemical Education*, **1996**, 73, 906. DOI: 10.1021/ed073p906

[40] O. Kahn, *Book Molecular Magnetism* Wiley, **1993**.

[41] S. Stoll, A. Schweiger, EasySpin, a comprehensive software package for spectral simulation and analysis in EPR, *Journal of Magnetic Resonance*, **2006**, 178, 42-55. DOI: 10.1016/j.jmr.2005.08.013

[42] Program APEX3, Bruker AXS Inc., Madison, WI, **2015**.

[43] G. Sheldrick, A short history of SHELX, *Acta Crystallographica Section A*, **2008**, 64, 112-122. DOI: 10.1107/S0108767307043930

[44] L. Farrugia, WinGX and ORTEP for Windows: an update, *Journal of Applied Crystallography*, **2012**, 45, 849-854. DOI: 10.1107/S0021889812029111

[45] Putz, H., and Brandenburg K., Diamond - Crystal and Molecular Structure Visualization, Crystal Impact, Kreuzherrenstr. 102, 53227 Bonn, Germany.

[46] B.G. Tabachnick, L.S. Fidell. Experimental Designs using ANOVA. Belmont, CA: Duxbury Press, **2007**.

[47] T. Ramasarma, The Emerging Redox Profile of Vanadium, *Proceedings of Indian National Science Academy*, **2003**, B69, 649-672.

[48] S. Li, Z. Li, J. Zhang, Z. Su, S. Qi, S. Guo, X. Tan, Polyoxometalate-based 3D porous framework with inorganic molecular nanocage units, *Journal of Chemical Sciences*, **2017**, 129, 573-578. DOI: 10.1007/s12039-017-1265-7

[49] A.W. Addison, T.N. Rao, J. Reedijk, J. van Rijn, G.C. Verschoor, Synthesis, structure, and spectroscopic properties of copper(II) compounds containing nitrogen–sulphur donor ligands; the crystal and molecular structure of aqua[1,7-bis(N-methylbenzimidazol-2′-yl)-2,6-

dithiaheptane]copper(II) perchlorate, *Journal of the Chemical Society, Dalton Transactions*, **1984**, 1349-1356. DOI: 10.1039/DT9840001349

[50] W. Yang, C. Lu, Q. Zhang, S. Chen, X. Zhan, J. Liu, Structure and Properties of a Novel 3D Straight-Channel Polyoxovanadate and an Unexpected Trimeric Barbiturate Obtained by Hydrothermal Reactions, *Inorganic Chemistry*, **2003**, 42, 7309-7314. DOI: 10.1021/ic034554p

[51] Z. Zhang, J. Guo, J. Fu, L. Zheng, D. Zhu, Y. Xu, Y. Song, Hydrothermal Syntheses and Crystal Structures of Two New Vanadium Phosphates, *Journal of Cluster Science*, **2012**, 23, 177-187. DOI: 10.1007/s10876-011-0385-3

[52] L.S.A. Dikshitulu, G.G. Rao, Titrimetric determination of vanadium(IV) with potassium permanganate at the room temperature, using phosphoric acid as catalyst and ferroin as internal indicator. *Fresenius' Zeitschrift für analytische Chemie*, **1962**, 189, 421-426. DOI: 10.1007/BF00497696

[53] I. D. Brown, D. Altermatt, Bond-valence parameters obtained from a systematic analysis of the Inorganic Crystal Structure Database. *Acta Crystallographica Section B*, **1985**, 41, 244-247. DOI: 10.1107/S0108768185002063

[54] R.L. Frost, K.L. Erickson, M.L. Weier, O. Carmody, Raman and infrared spectroscopy of selected vanadates, *Spectrochim Acta A*, **2005**, 61, 829-834. DOI: 10.1016/j.saa.2004.06.006

[55] M. Sawicka, P. Storoniak, P. Skurski, J. Błażejowski, J. Rak, TG-FTIR, DSC and quantum chemical studies of the thermal decomposition of quaternary methylammonium halides, *Chemical Physics*, **2006**, 324, 425-437. DOI: 10.1016/j.chemphys.2005.11.023

[56] M. Aureliano, D.C. Crans, Decavanadate ($V_{10}O_{28}^{6-}$) and oxovanadates: Oxometalates with many biological activities, *Journal of Inorganic Biochemistry*, **2009**, 103, 536-546. DOI: 10.1016/j.jinorgbio.2008.11.010

[57] I. Andersson, A. Gorzsás, C. Kerezsi, I. Tóth, L. Pettersson, Speciation in the aqueous $H^+/H_2VO_4^-/H_2O_2$/phosphate system, *Dalton Transactions*, **2005**, 3658-3666. DOI: 10.1039/B508273K

[58] D.C. Crans, J.J. Smee, E. Gaidamauskas, L. Yang, The Chemistry and Biochemistry of Vanadium and the Biological Activities Exerted by Vanadium Compounds, *Chemical Reviews*, **2004**, 104, 849-902. DOI: 10.1021/cr020607t

[59] N.I. Gumerova, and A. Rompel, Polyoxometalates in solution: speciation under spotlight, *Chemical Society Reviews*, **2020**, 49, 7568-7601. DOI: 10.1039/D0CS00392A

[60] A. Bencini, D. Gatteschi, *Book EPR of Exchange Coupled Systems*, Dover Publications, **2012**.

[61] A. Solé-Daura, A. Notario-Estévez, J.J. Carbó, J.M. Poblet, C. de Graaf, K.Y. Monakhov, X. López, How Does the Redox State of Polyoxovanadates Influence the Collective Behavior in Solution? A Case Study with $[I@V_{18}O_{42}]^{q-}$ (q = 3, 5, 7, 11, and 13), *Inorganic Chemistry*, **2019**, 58, 3881-3894. DOI: 10.1021/acs.inorgchem.8b03508

[62] M. Aureliano, Decavanadate Toxicology and Pharmacological Activities: V_{10} or V_1, Both or None?, *Oxidative Medicine and Cellular Longevity*, **2016**, 2016, 6103457. DOI: 10.1155/2016/6103457

[63] C. Daniel, H. Hartl, A Mixed-Valence V^{IV}/V^{V} Alkoxo-polyoxovanadium Cluster Series $[V_6O_8(OCH_3)_{11}]^{n+/-}$: Exploring the Influence of a μ-Oxo Ligand in a Spin Frustrated Structure, *Journal of the American Chemical Society*, **2009**, 131, 5101-5114. DOI: 10.1021/ja8073648

[64] K. Okaya, T. Kobayashi, Y. Koyama, Y. Hayashi, K. Isobe, Formation of V^{V} Lacunary Polyoxovanadates and Interconversion Reactions of Dodecavanadate Species, *European Journal of Inorganic Chemistry*, **2009**, 2009, 5156-5163. DOI: 10.1002/ejic.200900605

[65] P. Day, N.S. Hush, R.J.H. Clark, Mixed valence: origins and developments, *Philosophical Transactions of the Royal Society of London A: Mathematical, Physical and Engineering Sciences*, **2008**, 366, 5-14. DOI: 10.1098/rsta.2007.2135

[66] P. Day, Mixed-Valence Compounds, *Recherche*, **1981**, 12, 304-311.

[67] C. Daniel, H. Hartl, Neutral and Cationic V^{IV}/V^{V} Mixed-Valence Alkoxo-polyoxovanadium Clusters $[V_6O_7(OR)_{12}]^{n+}$ (R = $-CH_3$, $-C_2H_5$): Structural, Cyclovoltammetric and IR-Spectroscopic Investigations on Mixed Valency in a Hexanuclear Core, *Journal of the American Chemical Society*, **2005**, 127, 13978-13987. DOI: 10.1021/ja0529902b

[68] T.D. Keene, D.M. D'Alessandro, K.W. Krämer, J.R. Price, D.J. Price, S. Decurtins, C.J. Kepert, $[V_{16}O_{38}(CN)]^{9-}$: A Soluble Mixed-Valence Redox-Active Building Block with Strong Antiferromagnetic Coupling, *Inorganic Chemistry*, **2012**, 51, 9192-9199. DOI: 10.1021/ic3001834

[69] D. Marques-da-Silva, G. Fraqueza, R. Lagoa, A.A. Vannathan, S.S. Mal, M. Aureliano, Polyoxovanadate inhibition of Escherichia coli growth shows a reverse correlation with Ca^{2+}-ATPase inhibition, *New Journal of Chemistry*, **2019**, 43, 17577-17587. DOI: 10.1039/C9NJ01208G

[70] D. Althumairy, K. Postal, B.G. Barisas, G.G. Nunes, D.A. Roess, D.C. Crans, Polyoxometalates function as indirect activators of a G protein-coupled receptor, *Metallomics*, **2020**, 12, 1044-1061. DOI: 10.1039/D0MT00044B

[71] N. Samart, Z. Arhouma, S. Kumar, H.A. Murakami, D.C. Crick, D.C. Crans, Decavanadate Inhibits Mycobacterial Growth More Potently Than Other Oxovanadates, *Frontiers in Chemistry*, **2018**, 6. DOI: 10.3389/fchem.2018.00519

[72] O. Linnenberg, M. Moors, A. Solé-Daura, X. López, C. Bäumer, E. Kentzinger, W. Pyckhout-Hintzen, K.Y. Monakhov, Molecular Characteristics of a Mixed-Valence Polyoxovanadate $\{V^{IV/V}_{18}O_{42}\}$ in Solution and at the Liquid–Surface Interface, *The Journal of Physical Chemistry C*, **2017**, 121, 10419-10429. DOI: 10.1021/acs.jpcc.7b02138

[73] J. Geng, M. Li, J. Ren, E. Wang, X. Qu, Polyoxometalates as Inhibitors of the Aggregation of Amyloid β Peptides Associated with Alzheimer's Disease, *Angewandte Chemie International Edition*, **2011**, 50, 4184-4188. DOI: 10.1002/anie.201007067

[74] G. Zhang, B. Keita, C. Craescu, S. Miron, P. Oliveira, L. Nadjo, Polyoxometalate Binding to Human Serum Albumin: A Thermodynamic and Spectroscopic Approach, *The Journal of Physical Chemistry. B*, **2007**, 111, 11253-11259. DOI: 10.1021/jp072947u

[75] G. Zhang, B. Keita, C.T. Craescu, S. Miron, P. de Oliveira, L. Nadjo, Molecular Interactions between Wells−Dawson Type Polyoxometalates and Human Serum Albumin, *Biomacromolecules*, **2008**, 9, 812-817. DOI: 10.1021/bm701120j

[76] A. Solé-Daura, V. Goovaerts, K. Stroobants, G. Absillis, P. Jiménez-Lozano, J.M. Poblet, J.D. Hirst, T.N. Parac-Vogt, J.J. Carbó, Probing Polyoxometalate–Protein Interactions Using Molecular Dynamics Simulations, *Chemistry – A European Journal*, **2016**, 22, 15280-15289. DOI: 10.1002/chem.201602263

[77] I.S. Lee, J.R. Long, S.B. Prusiner, J.G. Safar, Selective Precipitation of Prions by Polyoxometalate Complexes, *Journal of the American Chemical Society*, **2005**, 127, 13802-13803. DOI: 10.1021/ja055219y

Highlights:

- Two mixed-valence octadecavanadates were synthesized and characterized.

- **$V_{18}P$** is $[\{K_6(OH_2)_{12}V^{IV}_{11}V^{V}_{7}O_{41}(PO_4) \cdot 4H_2O\}_n]$ and **$V_{18}I$** is $(NH_4)_2(Me_4N)_5[V^{IV}_{12}V^{V}_{6}O_{42}I] \cdot Me_4NI \cdot 5H_2O$.

- The chemoprotective activity of **$V_{18}P$** and **$V_{18}I$** against diethyl sulfate was assessed.

- **$V_{18}I$** counteracts the alkylating agent and provides 35% enhancement in culture growth.

- Halide-encapsulated POVs offer higher chemoprotection than phosphate analogs.